JYVÄSKYLÄ STUDIES IN BIOLOGICAL AND ENVIRONMENTAL SCIENCE 279

Ritika Sethi

Inter-domain Interactions in Filamins

Esitetään Jyväskylän yliopiston matemaattis-luonnontieteellisen tiedekunnan suostumuksella
julkisesti tarkastettavaksi yliopiston Ylistönrinteellä salissa YAA303
toukokuun 9. päivänä 2014 kello 12.

Academic dissertation to be publicly discussed, by permission of
the Faculty of Mathematics and Science of the University of Jyväskylä,
in Ylistönrinne, hall YAA303, on May 9, 2014 at 12 o'clock noon.

UNIVERSITY OF JYVÄSKYLÄ

JYVÄSKYLÄ 2014

Inter-domain Interactions in Filamins

JYVÄSKYLÄ STUDIES IN BIOLOGICAL AND ENVIRONMENTAL SCIENCE 279

Ritika Sethi

Inter-domain Interactions in Filamins

UNIVERSITY OF JYVÄSKYLÄ

JYVÄSKYLÄ 2014

Editors
Varpu Marjomäki
Department of Biological and Environmental Science, University of Jyväskylä
Pekka Olsbo, Timo Hautala
Publishing Unit, University Library of Jyväskylä

Jyväskylä Studies in Biological and Environmental Science
Editorial Board

Jari Haimi, Anssi Lensu, Timo Marjomäki, Varpu Marjomäki
Department of Biological and Environmental Science, University of Jyväskylä

Cover illustration: Ritika Sethi

URN:ISBN:978-951-39-5674-5
ISBN 978-951-39-5674-5 (PDF)

ISBN 978-951-39-5673-8 (nid.)
ISSN 1456-9701

Copyright © 2014, by University of Jyväskylä

Jyväskylä University Printing House, Jyväskylä 2014

"It is the mark of an educated mind to be able to entertain a thought without accepting it."
-Aristotle

"The mind is everything. What you think, you become"
-Buddha

ABSTRACT

Sethi, Ritika
Inter-domain interactions in filamins
Jyväskylä: University of Jyväskylä, 2014, 56 p.
(Jyväskylä Studies in Biological and Environmental Science
ISSN 1456-9701; 279)
ISBN 978-951-39-5673-8 (nid.)
ISBN 978-951-39-5674-5 (PDF)
Yhteenveto: Filamiini-proteiinien domeenien väliset vuorovaikutukset
Diss.

Filamins (FLNs) are large multi-domain proteins that cross-link filamentous actin and also act as a scaffold for various cytoskeletal, signaling and transmembrane proteins. Multiple studies have suggested that FLNs also function as mechanosensors in cells. In humans, there are three isoforms, FLNa, FLNb and FLNc. FLN mutations cause a spectrum of diseases that primarily affect the skeleton, brain and heart. Vertebrate FLNs are composed of an actin-binding domain (ABD) followed by a stretch of 24 immunoglobulin-like (Ig) domains. Domains 1-15 are termed as Rod 1 region and 16-24 as Rod 2 region. Previous studies have shown existence of three inter-domain interactions in the Rod 2 region that form the mechanosensor module in FLNs. Two of these interactions have been shown to negatively regulate ligand binding to these domains. On the other hand, Rod 1 region domains were predicted to be arranged in a linear manner. In this thesis, I have studied two hypotheses: (i) There are structural arrangements in the Rod 1 region that allow mechanosensing and (ii) the mechanosensor function of Rod 2 region is conserved also in Drosophila. For this, I first used low-resolution structural techniques to investigate if there were any inter-domain interactions in the Rod 1 region of FLNc. As a result, four compact regions were revealed, FLNc3-4, 4-5, 11-12 and 14-15. Crystal structures of FLNa3-5 and FLNc4-5 showed novel type of interactions between Ig domains. Next we showed that domain 4 is able to bind a ligand and domain 5 stabilizes the structure of domain 4. Hence, in context of FLN3-5 module, the inter-domain interactions seem to positively regulate ligand binding. To study the structural conservation of the Rod 2 region, mutations that affect the mechanical properties of human FLNs were introduced in the *Drosophila melanogaster* orthologue protein Cher. Low-resolution scattering techniques showed that the overall structure of Cher mechanosensor region was similar to that of human and that the open mechanosensor mutant significantly altered the structure.

Keywords: Crystallography; inter-domain interactions; filamins; immunoglobulin-like domains; mechanosensor; small angle x-ray scattering.

Ritika Sethi, University of Jyväskylä, Department of Biological and Environmental Science, P.O. Box 35, FI-40014 University of Jyväskylä, Finland.

Author's address Ritika Sethi
Department of Biological and Environmental Science
P.O. Box 35
FI-40014 University of Jyväskylä
Finland
ritika.sethi@jyu.fi

Supervisor Professor Jari Ylänne
Department of Biological and Environmental Science
P.O. Box 35
FI-40014 University of Jyväskylä
Finland

Reviewers Adjunct Professor Tassos Papageorgiou
Turku Centre for Biotechnology,
Biocity Turku, 5th floor, Tykistokatu 6,
Turku 20521
Finland

Professor John Trinick
School of Molecular and Cellular Biology
University of Leeds
Leeds
LS2 9JT
United Kingdom

Opponent Assistant Professor Fumihiko Nakamura
Translational Medicine Division,
Department of Medicine,
Brigham and Women's Hospital,
Harvard Medical School,
Boston, MA 02115
United States

CONTENTS

LIST OF ORIGINAL PUBLICATIONS

This thesis is based on the following publications. These will be referred to in the thesis by roman numerals.

I: Sethi, R., and Ylänne, J. Small angle x-ray scattering reveals compact domain-domain interactions in the N-terminal region of filamin C. Submitted manuscript.

II: Sethi, R., Seppälä, J., Tossavainen, H., Ylilauri, M., Ruskamo, S., Pentikäinen, O.T., Pentikäinen, U., Permi, P., and Ylänne, J. 2014. A novel structural unit in the N-terminal region of filamins. *Journal of Biological Chemistry,* 289: 8588-8598.

III: Sethi, R., Huelsmann, S., and Ylänne, J. Biophysical evidence for structural and functional conservation of filamin mechanosensor domains between human and *Drosophila melanogaster* (manuscript).

CONTRIBUTION OF RITIKA SETHI IN THE ARTICLES

Article I — I performed ligation independent cloning, protein expression, purification. I collected and analyzed the small angle x-ray scattering (SAXS) data. I prepared the figures and wrote the manuscript with Jari Ylänne.

Article II — I cloned, expressed and purified FLNc4-5 and all the mutants. I collected SAXS data on FLNc4-5 with Salla Ruskamo and on the mutants by myself. I processed all the data and built the models. I crystallized FLNc4-5 and collected the diffraction data. I processed the data and solved the structure with Jari Ylänne. I co-crystallized FLNc4-5/GPIb and collected the diffraction data. I processed the data and solved the structure with Jari Ylänne. I performed the pull-down and thermofluor assays. I also cloned, expressed and purified labeled FLNc4-5 and FLNc5 for NMR measurements with help from Arja Mansikkaviita. I prepared the figures and wrote the manuscript with contribution from all the co-authors.

Article III — I cloned, expressed and purified the proteins. I collected and processed the SAXS data. I wrote the manuscript with Jari Ylänne.

ABBREVIATIONS

F-actin	Filamentous-actin
FLNs	Filamins
ABD	Actin binding domain
H1 and H2	Hinge 1 and Hinge 2
CH	Calponin homology
ABS	Actin binding site
ECM	Extracellular matrix
Ig	Immunoglobulin-like
FLNa	Filamin A
FLNb	Filamin B
FLNc	Filamin C
GPIbα	Glycoprotein Ibα
SAXS	Small Angle X-ray Scattering
NMR	Nuclear Magnetic Resonance
MD	Molecular dynamics
D_{max}	Maximum Dimension
R_g	Radius of Gyration
OPD	Otopalatodigital
PVNH	Periventricular Nodular Heterotopia
BD	Boomerang Dysplasia
LS	Larsen Syndrome
SCT	Spondylocarpotarsal
MFMs	Myofibrillar Myopathies

1 INTRODUCTION

Actin cytoskeleton is crucial for the formation and maintenance of cell shape and morphology. Processes like cell migration, spreading, cell -cell adhesion and cell-extra-cellular matrix (ECM) adhesion, are all dependent on the dynamic manipulation of the actin network in response to external or internal stimuli (Lee and Dominguez, 2010; Stossel *et al.*, 2001). Actin remodeling is regulated by many different actin-binding proteins. Filamins (FLNs) are one such family of actin binding proteins that cross-link filamentous actin (F-actin). They are large, flexible, multi-domain proteins that cross-associate the actin filaments at varying angles (Hartwig *et al.*, 1980). In addition, FLNs act as a scaffold for many proteins including transmembrane receptors, ion channels, intra-cellular signaling proteins and cytoskeletal regulators (Stossel *et al.*, 2001; Nakamura *et al.*, 2011). Hence, they are crucial in the development of tissues and organs and patient mutations in FLNs exhibit a wide spectrum of phenotypes (Fürst *et al.*, 2012; Kley *et al.*, 2012) .

This thesis investigates the structure of FLNs and its effect on the regulation of ligand binding. To that end, low-resolution structures of the N-terminal two-domain fragments of FLNc were obtained (I). Atomic structures of two fragments from the N-terminal of FLNa and FLNc were solved (II). And finally, in order to understand if the C-terminal mechanosensitive region of FLNs is structurally and functionally conserved in *Drosophila* and humans, low-resolution structural parameters of a five-domain fragment were compared (III).

In depth structural characterization of FLNs is crucial in understanding its functions as a mediator of the visco-elastic properties of actin network. This work has primarily focused on the structural aspects of FLN domain organization while striving to extrapolate the results to FLN function in cells.

2 REVIEW OF THE LITERATURE

2.1 Filamins

Since their discovery in rabbit alveolar macrophages in 1975 (Hartwig *et al.*, 1975) several reports have confirmed the existence of FLNs throughout the animal kingdom, including *Drosophila melanogaster* (fruit fly) (Sokol and Cooley, 1999) and *Caenorhabditis elegans* (round worm) (Kovacevic and Cram, 2010). Shorter FLN like proteins have also been reported in amoeba like *Entamoeba histolytica* (parasite) (Vargas *et al.*, 1996) and *Dictyostelium discoidium* (slime mold) (Hock and Condeelis, 1987). In humans, there are three FLN paralogues, *FLNA*, *FLNB* and *FLNC,* with a conserved intron-exon pattern that expresses proteins (FLNa, FLNb and FLNc) (Van Der Flier and Sonnenberg, 2001). While *FLNA* and *FLNB* are expressed ubiquitously in many different cell types, *FLNC* is expressed only in cardiac and skeletal muscles (Van der Flier and Sonnenberg, 2001). The molecular weight of human FLN proteins ranges from 276 - 289 kDa (Gorlin *et al.*, 1990; Stossel *et al.*, 2001; Xie *et al.*, 1998; Xu *et al.*, 1998)

Knock out mouse models for all three *FLN* isoforms have been reported (Bicknell *et al.*, 2007; Dalkilic *et al.*, 2006; Farrington-Rock *et al.*, 2008; Feng *et al.*, 2006; Hart *et al.*, 2006; Krakow *et al.*, 2004; Leung *et al.*, 2010; Lu *et al.*, 2007; Zhou *et al.*, 2007). *FLNA* deficient mice showed various developmental defects in heart, brain and skeleton, similar to those of otopalatodigital syndrome (OPD) and cardiac valvular dystrophy in humans caused by missense mutations in *FLNA* (Zhou *et al.*, 2007; Hart *et al.*,2006; Kyndt *et al.*, 2007). In mice, while monocytes derived from the bone marrow showed problems with migration (Leung *et al.*, 2010), the fibroblasts, neurons (Hart *et al.*, 2006) and endothelial cells (Feng *et al.*, 2006) showed normal motility. Also, one of the most striking observations was abnormal vasculature, possibly an attribute of reduced VE-cadherin levels in endothelial and neuroepithelial cells (Feng *et al.*, 2006). Similarly, *FLNB* deficiency in mice is embryonically lethal with severe skeletal malformations of the vertebrae, sternum, and reduced cartilage in the carpal

and tarsal bones (Farrington-Rock *et al.*, 2008; Zhou *et al.*, 2007; Bicknell *et al.*, 2007). FLNb deficient chondrocytes showed reduced adhesion to the ECM due to loss of FLNb-integrin-β1 linkages (Lu *et al.*, 2007). These phenotypes are similar to those of boomerang dysplasia (BD) and spondylocarpotarsal syndrome (SCT) in humans and suggested a role of FLNb in cartilage development (Bicknell *et al.*, 2007; Krakow *et al.*, 2004). *FLNC* deficiency causes postnatal respiratory failure and reduced number of muscle fibers. These phenotypes are consistent with that of human myofibrillar myopathies (MFMs) and emphasize the role of FLNc in muscle development and maintenance (Dalkilic *et al.*, 2006). Altogether, these results suggested that both cell motility and scaffolding functions of FLNs may play a role in the disease phenotype.

2.1.1 Overall architecture of human filamins

As cross-linkage of actin requires presence of two actin binding domains (ABD), all FLNs exist as homodimers, where each subunit consists of an ABD at the N-terminus followed by a long string of 24 immunoglobulin-like (Ig) domains (Figure 1) (Gorlin *et al.*, 1990; Van der Flier and Sonnenberg, 2001). Ig domains 1 -15 are referred to as Rod 1 region followed by a protease sensitive flexible hinge of 25 residues known as hinge 1 (H1). Following H1there are domains 16-24 that are referred to as Rod 2 region. In Rod 2, there is a second flexible hinge of 35 residues (H2) between domains 23-24 and domain 24 is the domain responsible for formation of the dimer (Pudas *et al.*, 2005). The presence of the flexible hinges and the dimerization domain gives FLNs their characteristic V or Y shape (Gorlin *et al.*, 1990). The overall sequence of the rod region is highly conserved between different isoforms with approximately 70% homology (Van der Flier and Sonnenberg, 2001) with the exception of FLNc, where there is an extra stretch of 81 residues in domain 20 (Xie *et al.*, 1998), which has been shown to play a role in the sarcomeric Z-disk targeting of FLNc (van der Ven *et al.*, 2000). On the other hand, the hinge regions are not well conserved and share only 45% sequence homology between isoforms (Van der Flier and Sonnenberg, 2001). For example, H1 is missing from some FLNb transcription variants and also from FLNc (Van der Flier and Sonnenberg, 2001). Rotary shadowing electron micrographs have showed each filamin monomer to be around 80 nm long (Gorlin *et al.*, 1990; Van der Flier and Sonnenberg, 2001) and recent studies have indicated (Nakamura, *et al.* 2007) that Rod 1 region itself is around 57 nm in length suggesting it to be composed to a string of Ig domains connected in a tail to head fashion. On the other hand, Rod 2 region seems to be compact measuring around 20 nm in length (Nakamura, *et al.* 2007).

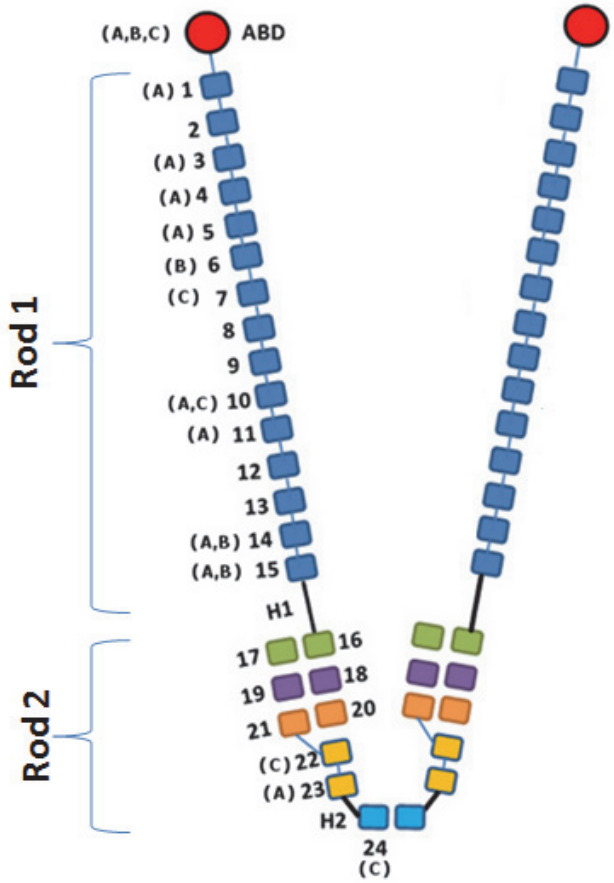

FIGURE 1 Filamin dimer model: ABDs are shown in red, followed by 24 Ig domains. Rod 1 and Rod 2 regions are marked. The three known inter-domain interactions in the Rod 2 region (FLN16-17, FLN18-19 and FLN20-21) are shown in green, purple and orange, respectively. Isoform specific (*FLNA*, *FLNB* and *FLNC*) mutations in human patients are shown on the left subunit.

2.1.2 Filamin actin binding domain

The actin binding domain of FLNs is similar to that of α-actinin ABD (Bañuelos *et al.*, 1998). It is composed of two calponin-homology (CH1 and CH2) domains (Figure 2) of 110 residues each that are connected by a flexible linker. Each CH domain has 6 α helices, 4 of which are major and 2 are short. 3 of the 4 major helices form a helical bundle against which the 1st α helix aligns in a perpendicular orientation. All helices are connected by long loops. The angle between the two consecutive CH domains is determined by the last α helix of the CH1 domain (Ruskamo and Ylänne, 2009). Mutation and biochemical studies have revealed three actin-binding sites (ABS) in ABDs. ABS1 and ABS2 are mapped to the 1st and the last α helix of the CH1 domain, respectively while ABS3 is located on the 1st α helix of the CH2 domain. The ABS2 seems to be

crucial for F-actin binding ability of the domain whereas ABS3 is required for the avidity (Bresnick *et al.*, 1991; Van Der and Sonnenberg, 2001; Kuhlman *et al.*, 1992). In FLNs, recent studies have also suggested that there is a second actin binding site between domains 9-15 which facilitates the binding of the F-actin to Filamin (Nakamura *et al.*, 2007). Several patient mutations (Figure 1) causing otopalatodigital syndrome (OPD), periventricular nodular heterotopia (PVNH) (Robertson *et al.*, 2003), Larsen Syndrome (LS) and Boomerang Dysplasia (BD) (Krakow *et al.*, 2004) have been mapped at the ABD of FLNa.

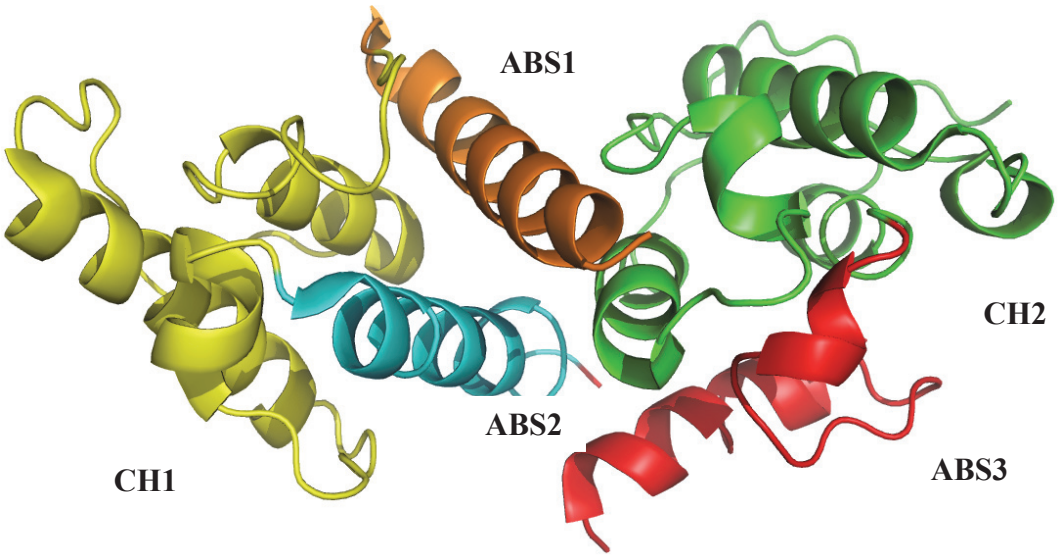

FIGURE 2 Crystal structure of the ABD: α helices shown in yellow, cyan and orange comprise CH1 and the helices in green and red are CH2. The first α helix of CH1 containing the ABS1 is shown in orange, ABS2 is shown in cyan and ABS3 located on the 1st α helix of the CH2 domain is shown in red. Notice the perpendicular orientation of the 1st α helix from each domain (orange and red) with respect to the helical bundle.

2.1.3 Filamin immunoglobulin-like domains

According to the structural classification of proteins (SCOP) database, all Ig domains in FLNs fit under the E subtype of Ig domain family (Pudas *et al.*, 2005). In this subtype, each domain has 7 β-strands (A-G) made up of 6-10 amino acids each (Figure 3A). β-strands A, B, E and D form one β sheet that is aligned anti-parallel to the second β sheet comprising of β-strands C, F and G. This β sandwich fold is conserved in all the human FLNs. Each domain is approximately 100 residues (Gorlin *et al.*, 1990; Van der Flier and Sonnenberg, 2001) and has dimensions of approximately 4.0-4.8 nm x 2.0-2.6 nm x 1.5-1.8 nm (Nakamura *et al.*, 2007). In most of the single domain structures of FLNs

(solution NMR or crystal) available in the protein database, there is a characteristic 3_{10} helix in the A strand (Figure 3A) with a consensus sequence of GXG (where X is either Proline or Arginine or Leucine). This helix interrupts the β-strand A, thereby leading to a shorter β-strand A' prior to strand B (PDB ID: 2D7M, 2DI8, 2BP3 (Nakamura *et al.*, 2006), 2W0P (Lad *et al.*, 2008), 2NQC (Sjekloca *et al.*, 2007), 2DI9, 2DIA, 2DMB, 3CNK (Seo *et al.*, 2009), 2DJ4, 2DIB, 2DIC and 4B7L (Sawyer *et al.*, 2012)). Interestingly, in some FLN domains where the GXG motif is not present, the A strand is not folded in with the rest of the domain. Such structures are FLNc16 (PDB ID: 2D7N), FLNb18 (PDB ID: 2DMC) (Figure 3B) and FLNb20 (PDB ID: 2DLG).

Similar to ABD mutations, patient mutations in FLN Ig domains have also been identified that cause a spectrum of disorders like PVNH (Zenker *et al.*, 2004), OPD (Robertson *et al.*, 2003), X linked Cardiac Valvular Dysplasia (Kyndt *et al.*, 2007), Larsen Syndrome (Bicknell *et al.*, 2007; Krakow *et al.*, 2004) and myofibrillar myopathies (MFM) (Luan *et al.*, 2010; Shatunov *et al.*, 2009; Vorgerd *et al.*, 2005).

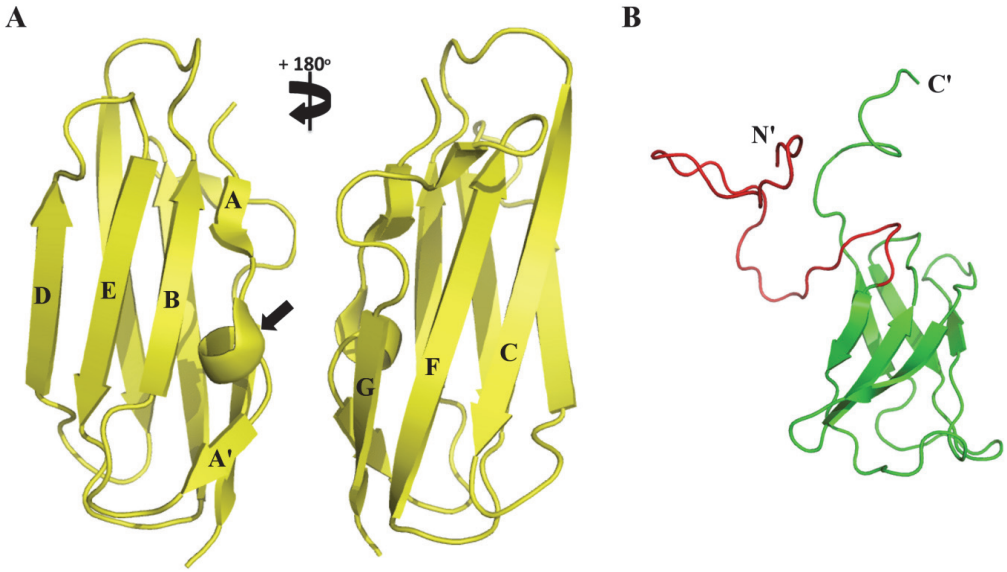

FIGURE 3 (A) Crystal structure of FLNa17 from PDB ID: 2BP3 showing the typical β sheet topology of Ig domains. β sheet comprising β-strands ABED is shown on the left side in the panel. The 3_{10} helix in the A strand is marked with an arrow. Right side of the panel shows the β-strands CFG. (B) Solution NMR structure of FLNb18 (PDB ID: 2DMC) showing the unfolded A strand in red.

2.2 Known domain-domain interactions of Filamins

Large multi-modular proteins are generally thought to be composed of domains that work independently of each other like beads on a string. FLNs do not seem to conform to this outlook. Although they are flexible proteins composed of 24 similar Ig domains, some functional inter-domain interactions have been reported in the Rod 2 region of FLNs.

2.2.1 Domain pair 16-17

SAXS and NMR experiments have revealed inter-domain interactions between FLNa domains 16 and 17 (Heikkinen *et al.*, 2009). Similar to the single domain structure of FLNc16 (PDB ID: 2D7N), the first β-strand of FLNa16 is also detached from the rest of the domain in this domain pair structure (Figure 4). This leads to exposure of a hydrophobic core around the β-strands B-G (BG face) of domain 16, which then bind tightly to the β-strands A-G of domain 17. This interaction is mainly hydrophobic and causes the β sheets of both domains to stack in parallel, hence leading to a large interaction surface area of around 720 Å^2.

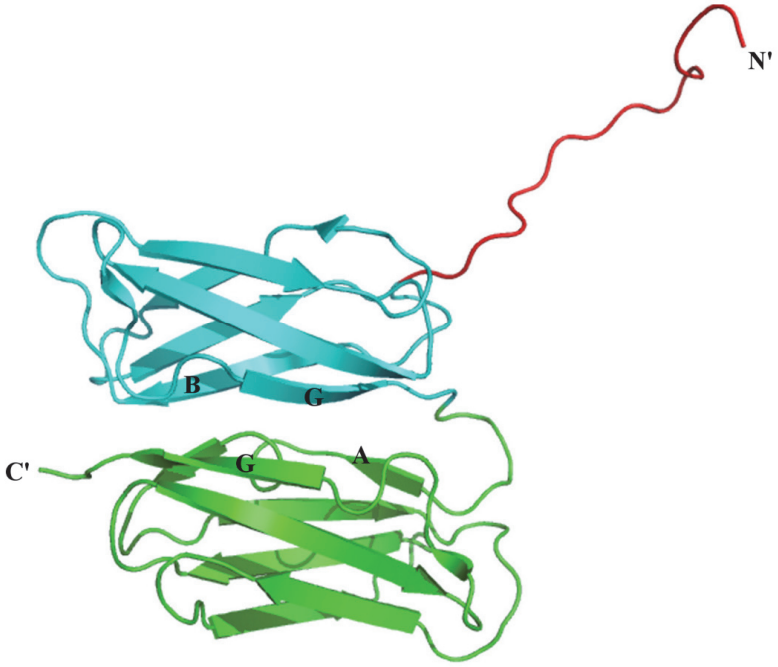

FIGURE 4 Structure of FLNa16-17 derived from PDB ID: 2K7P. Domain 16 is cyan and domain 17 is green. The unfolded A strand of domain 16 is shown in red. The β-strands at the domain-domain interface are marked.

2.2.2 Domain pair 18-19

The structure of FLNa18-19 (Figure 5) domain pair was solved with NMR (Heikkinen *et al.*, 2009). Although the A strand of domain 18 is detached from the rest of the domain, like in domain 16, the mode of interaction between the two domains is different from that of FLNa16-17. Here, the A strand detachment from domain 18 leads to exposure of the hydrophobic core at the BG face which is then filled by the tyrosine 2077 (TYR 2077) located at the BC loop of domain 19. This orientates the two domains in an orthogonal fashion. Also, the A strand of domain 18 forms main chain hydrogen bonds with the strand C and interacts with the hydrophobic cavity between strands C and D of domain 19. This interface is called the CD face. The interaction creates an extra β-strand, thereby extending the β sheet CFG. In addition, there are also some side chain hydrogen bonds between the A strand of domain 18 and the D strand of domain 19. The buried area at the A strand interface itself is around 600 Å^2.

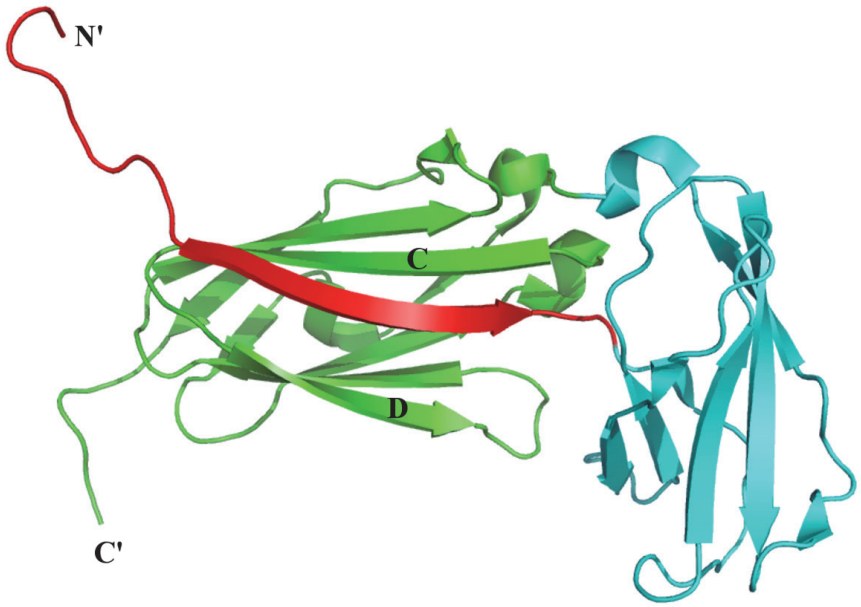

FIGURE 5 Structure of FLNa18-19 derived from PDB ID: 2K7Q. Domain 18 is cyan and domain 19 is green. The A strand of domain 18 is shown in red. The β-strands CD of domain 19 are marked.

2.2.3 Domain pair 20-21

The crystal structure of the triplet of FLNa domains 19-21 was the first structure revealing inter-domain interactions in vertebrate FLNs (Lad *et al.*, 2007). It showed that in human FLNs, the organization of the domains is not sequential as seen in *Dictyostelium* (Popowicz *et al.*, 2004). Since the atomic details of FLNa18-19 interactions have been mentioned earlier, only the domain-domain interactions of FLNa20-21 (Figure 6) will be discussed here. As in the domain pair of 18-19, the A strand of domain 20 also extends away from the domain and attaches to the groove at the CD face of domain 21. Here, the interaction mechanism is similar to that of FLNa18-19. However, the perpendicular orientation of domain 20 on top of domain 21 is attributed mostly to the interactions between the β-strand G of domain 20 and BC loop of domain 21. The buried area at CD face interface is around 727 Å^2.

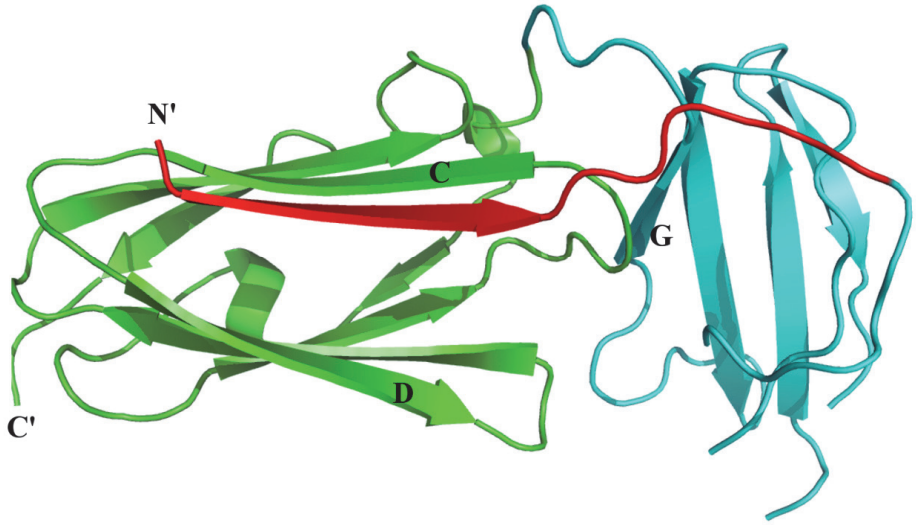

FIGURE 6 Crystal structure of FLNa20-21 derived from PDB ID: 2J3S. Domain 20 is cyan and domain 21 is green. The A strand of domain 20 is shown in red. The β-strands CD of domain 21 and the β-strand G of domain 20 are marked.

2.2.4 Human FLN dimerization

Dimerization of FLN monomers is essential for FLN actin cross-linking function (Gorlin *et al.*, 1990). The first crystal structure showing the details of the dimerization interface for human FLNs was solved for FLNc24 (Pudas *et al.*, 2005) (Figure 7). Here, single domains 24 interacted extensively with each other at the CD face leading to a large buried interface area of 1109 Å^2. This interaction is attributed to the formation of six hydrogen bonds between β-strands D of each domain and hydrophobic stacking of methionine and glycine

at the β-strands C from each domain. This leads to the formation of a continuous anti- parallel β sheet containing 8 β-strands. It is interesting to note that although the interaction here is mediated by the CD face, the β sheet augmentation occurs via strand D rather than strand C. The crystal structure of FLNa24 that was solved later, also showed similar dimerization pattern (Seo *et al.*, 2009).

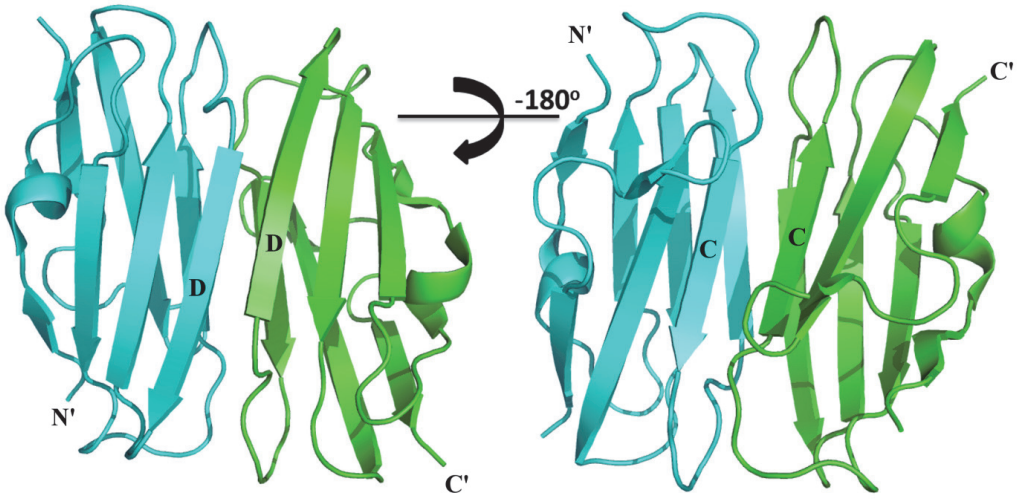

FIGURE 7 Crystal structure of FLNc dimerization from PDB ID: 1VO5. One domain is cyan and the other is green. The left side shows one view of the interface with β-strands D from each domain aligned in anti-parallel orientation. The right side shows the interface at 180° rotation with β-strands C from each domain aligned in anti-parallel orientation.

2.3 Structural basis of Filamin-ligand interactions

Filamins are known to interact not only with actin filaments, but also with a range of binding partners including transmembrane proteins, signaling molecules and cytoskeletal proteins (Stossel *et al.*, 2001). Most of these interactions seem to occur at the C terminal Rod 2 region. Because of its large size and flexibility, full-length structures of FLNs are not available. However, in the recent years, there has been a substantial increase in the number of structural and biochemical studies involving shorter fragments of FLN that have revealed the atomic details of how FLNs exhibit their interactions with some of the binding partners. In this section, only the FLN interactions where high-resolution structures are available are discussed.

2.3.1 Transmembrane adhesion proteins

Filamins interact with the cytoplasmic tails of the transmembrane adhesion proteins, Integrin β subunits and platelet Glycoprotein Ibα (GPIbα) (Meyer *et al.*, 1997; Pfaff *et al.*, 1998; Xu *et al.*, 1998). Many of the cell functions like cell migration, spreading, cell-cell and cell-extracellular matrix (ECM) signaling are regulated by a complex interplay between the extracellular matrix, transmembrane proteins, cytoskeleton, and intracellular signaling molecules. Integrins are one such key integrators of signaling that allow bi-directional flow of biochemical and mechanical cues (Hynes, 2002). Similarly, GPIbα is one of the components of the platelet von Willebrand factor (vWF) receptor complex which is required for normal platelet activation and function (López, 1994). FLNs may be involved in stabilization of these receptors on the plasma membrane via multiple different mechanism (Meyer *et al.*, 1998; Williamson *et al.*, 2002) . The main function of FLN-adhesion receptor interaction seems to be involvement in signaling. In the case of integrins, FLNs negatively regulate integrin activation by competing with another cytoskeletal protein talin, which is the main positive regulator of integrins (Kiema *et al.*, 2006; Tadokoro *et al.*, 2003). Both, talin and filamins, compete for the same binding site on the cytoplasmic tail of β integrin (Kiema *et al.*, 2006). Loss and gain of function mutations have suggested a FLN brake-like mechanism where FLN binding to β integrin cytoplasmic domain is required for efficient cell migration but a stronger interaction between the two reduces the cell motility (Calderwood *et al.*, 2001). In the context of platelet function, FLNa association with GPIbα is the essential first link that connects the chain of signaling proteins required for efficient platelet adhesion to vWF under high shear (Feng *et al.*, 2003).

These studies are further buttressed by biochemical and structural data confirming the sites for these interactions in FLNs, β integrins and GPIbα. Pull-down assays showed that while both, FLNa19 and 21, can interact with β7 integrins, domain 21 has a higher affinity (Kiema *et al.*, 2006). The crystal structure of β7 and β2 integrin peptide bound to FLNa21 (Kiema *et al.*, 2006; Takala *et al.*, 2008) then revealed the atomic details of this interaction where the interacting residues of integrin form an anti-parallel β-strand next to the strand C at the CD face of domain 21. Similarly, the binding site for GPIbα was mapped at FLNa17-19 (Meyer *et al.*, 1997) and within this fragment, FLNa17 was shown to have the highest affinity (Nakamura *et al.*, 2006). The crystal structure of FLNa17 in complex with GPIbα peptide then showed that residues 560-573 of the peptide bind at the CD face of FLNa17 in a similar manner as in case of FLN-integrin interaction (Nakamura *et al.*, 2006). In addition, there is ample evidence suggesting that both integrins and GPIbα bind multiple sites in FLNs, like domains 4, 9, 12, 17, 19, 21 and 23 (Ithychanda *et al.*, 2009).

2.3.2 Ion channels

Cystic fibrosis is a hereditary autoimmune disorder characterized by impaired chloride ion gating that leads to high chloride ion concentration in sweat,

accumulation of mucus in lungs, and respiratory infections (Gadsby *et al.*, 2006). The disease is mainly caused by ΔF508 mutation in the chloride ion channel protein called cystic fibrosis transmembrane conductance regulator (CFTR). The mutated protein is abnormally folded, which causes its retention in the endoplasmic reticulum and inefficient trafficking to the plasma membrane of epithelial cells (Sharma *et al.*, 2004). FLNa binds to the N -terminus of CFTR (Thelin *et al.*, 2007). The S13F mutation in CFTR protein is also one of the documented causes of cystic fibrosis and has been linked to its inability to bind FLNs and therefore its reduced expression at the membrane. Smith and coworkers (Smith *et al.*, 2010) have explained the biochemical basis of the FLN-CFTR interaction using structural techniques. They have determined the FLN binding site on CFTR to be residing between residues 10-19 and emphasized on the importance of S13 residue that makes several hydrogen bonds with the strand C at the CD face of FLN domain 21. Playford and colleagues (Playford *et al.*, 2010) have then showed using pull-down assays that CFTR peptide can interact with multiple domains in FLNa, i.e domains 9, 12, 17, 19, 21 and 23. The interaction, once again resembles that of the previously discussed FLN-integrin and FLN-GPIbα, although the affinities are lower, ostensibly expediting the dynamic clustering of CFTR at the membrane (Playford *et al.*, 2010).

2.3.3 Adhesion adaptor protein

Migfilin is a LIM-domain containing adaptor protein that localizes near the actin cortex and links the actin cytoskeleton to the integrin-ECM contacts (Tu *et al.*, 2003). As mentioned earlier, the simultaneous association of integrin receptors with the ECM ligands and with the cytoskeleton is an important step in regulation of cell migration and adhesion. Migfilin has been reported to promote the talin associated integrin activation by binding to filamin and in turn disrupting its interaction with integrin (Ithychanda, Das, *et al.*, 2009). Functional studies have shown that residues 1-85 from the N-terminal region of migfilin bind to FLNa and FLNc between domains 19-24 (Tu *et al.*, 2003). NMR studies with migfilin deletion mutants aided in demarcating the precise binding region to be located between the first 24 residues (Lad *et al.*, 2008; Ithychanda *et al.*, 2009). Pull-down assays with His-tagged migfilin and single FLN domains showed that migfilin binds to FLNa21with the highest affinity (Lad *et al.*, 2008). In the same paper, the crystal structure of migfilin bound to domain FLNa21 showed that the mode of interaction is similar to that of the previously characterized FLNa21-integrin β7 involving contacts between Pro^{5} - Pro^{19} of migfilin and CD face of FLNa21.

2.3.4 Common mechanism of ligand binding

The aforementioned complex structures have provided valuable data to understand the mechanism by which the FLN Ig domains bind multitude of ligands. Strikingly, there seems to be a common mode of interaction where individual domains act as interaction modules. They interact with other

proteins using a β sheet augmentation mechanism. Here, the interaction partner forms an additional β-strand in anti-parallel orientation next to the strand C of the FLN domain and simultaneously interacts with the hydrophobic alcove between the strands C and D, referred to as the CD face. Up to nine amino acids from the ligand corresponding to a typical β-strand forming motif and containing alternating hydrophobic residues, form main chain hydrogen bonds with the β-strand C of the FLN Ig domain. Hence, the driving mechanism of the interactions is primarily attributed to the main chain hydrogen bonding but the specificity is provided by the side chain interactions of five residues of the binding peptide with the cavity between the strands C and D (Razinia *et al.*, 2012). The pattern (shown in Figure 8 and Table I) is such that the first of these residues is either aliphatic or aromatic and the side chain points towards the CD loop. The second residue is a serine that seems to be conserved in all the mentioned binding partners and is hydrogen bonded to the β-strand D of the Ig domain. The following two residues are either aliphatic or aromatic and are buried in the hydrophobic groove. The fifth amino acid is usually aliphatic and points towards the BC loop of the Ig domain.

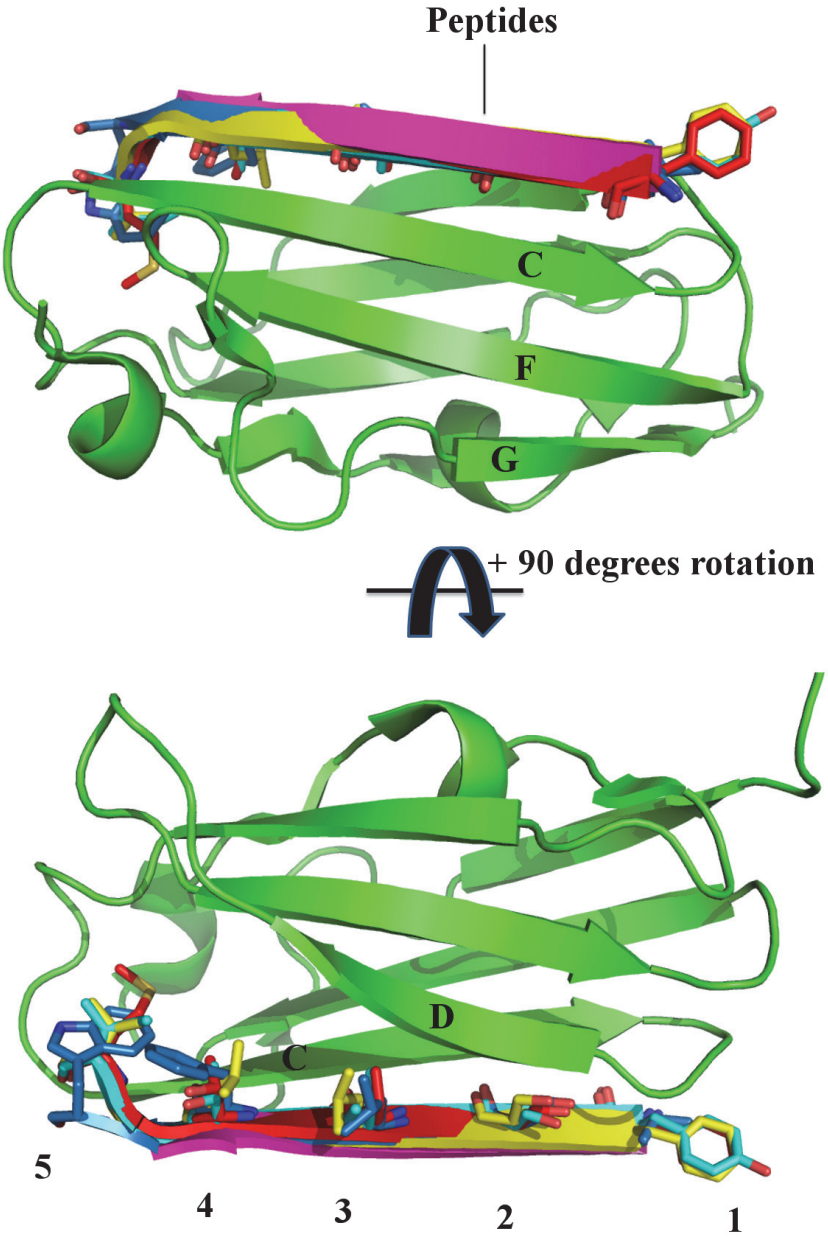

FIGURE 8 FLNa21 (green) with the superimposed ligand peptides of GPIbα (yellow), Migfilin (pink), Integrin β7 (cyan), Integrin β2 (red) and CFTR (blue). Top panel shows how peptides form an anti-parallel β-strand next to the strand C of domain 21 at the CD face. Lower panel shows the orientation of the side chains of the five residues of the binding peptides that interact with the cavity between the strands C and D of FLNa21.

TABLE 1: Alignment of the ligand residues that interact with the CD face of FLN Ig domains[$]

	1[#]		**2[#]**		**3[#]**		**4[#]**		**5[#]**
Integrin β7	Y	K	S	A	I	T	T	T	I
Integrin β2	F	K	S	A	T	T	T	V	M
GPIbα	F	R	S	S	L	F	L	W	V
CFTR	V	V	S	K	L	F	F	S	W
Migfilin	V	A	S	S	V	F	I	T	L

[$]Adapted from Razinia *et al.*, 2012 (Razinia *et al.*, 2012)

[#] Numbers 1-5 in the first row refer to the peptide residues pointing towards the CD face

Similar mechanism of interaction for FLN binding GTPase-activating protein (FILGAP) and FLN domain 23 was confirmed by pull-down and chemical shift assays (Nakamura *et al.*, 2009).

In addition to the above mentioned interaction partners, there are many FLN ligands (Nakamura *et al.*, 2011), some of which do not correspond to an obvious β-strand forming motif (Li *et al.*, 2000) and for some, the interacting sequences are not known yet. Hence, it is likely that there are other mechanisms by which FLNs interact with ligands.

2.4 Mechanosensing function of Filamins

Mechanosensing has emerged as a universal mechanism to regulate multicellular development (Ricca *et al.*, 2013). Cells grow in a highly dynamic environment where they are constantly subjected to mechanical forces or constraints. Cells are capable of sensing these mechanical inputs and respond by shape changes, adhesion, migration, protein expression, proliferation and differentiation. There are two aspects of mechanosensing, i.e rigidity sensing (Moore *et al.*, 2010) (as in cells generate forces to pull on the ECM for stiffness probing) and force sensing (Glogauer *et al.*, 1997) (cells perceive the externally applied force). These two aspects are difficult to distinguish as they may occur simultaneously and use similar cellular machinery (Puklin-Faucher and Sheetz, 2009).

Actin cytoskeleton is a key shared component of force and rigidity sensing. Studies have shown that force causes a) formation of focal adhesions at the cell-ECM junction; b) crosslinking of actin filaments along the stress fibers and near cytoskeleton-membrane edge; and c) actin filament assembly and treadmilling at the leading edge of the cell (Rossier *et al.*, 2010). In other words,

force modifies the interactions of actin-associated proteins that provide feedback signals to strengthen the cytoskeleton architecture. Five non-covalent interactions can be identified in this feedback cascade, ie. actin-myosin binding, formation of actin filaments from actin monomers, binding of actin filaments to linker proteins, binding of linker proteins to integrin and finally the binding of integrin to ECM ligands (Moore *et al.*, 2010). In addition to these, protein kinases and small GTP binding proteins are also involved in signaling (Gardel *et al.*, 2010) and the signals are also transmitted to the nucleus, thereby affecting gene expression (Wang *et al.*, 2009). In the context of the cytoskeletal linker proteins, there are many potential force-sensitive proteins. The best characterized candidates are talin, vinculin, α actinin, titin and filamin (Moore *et al.*, 2010). In this section, I will focus on the evidence and the potential mechanism of filamin mechanosensing.

Because filamins are one of the most potent F-actin cross linkers (Brotschi *et al.*, 1978) and known to localize near the membrane and at the focal adhesions, it is possible that they are heavily involved in the mechanical signaling cascade (Glogauer *et al.*, 1998; Nikki *et al.*, 2002; Stossel *et al.*, 2001). Experiments based on fluorophore labeling of force exposed cysteines in cytoskeletal proteins revealed that FLNs undergo conformational change upon force application (Johnson *et al.*, 2007). *In vivo* experiments have indicated increased expression levels of FLNa in cells where force is applied via β1 integrins (D'Addario *et al.*, 2001) and also increased recruitment of FLNs to the site of force application (Glogauer *et al.*, 1998). Glogauer et al (Glogauer *et al.*, 1998) have showed that FLN is required for reinforcement of adhesion sites when force is applied via integrin receptors, thereby suggesting its role in mechanoprotection. There are also data supporting the role of FLN in rigidity sensing. The FLNa- β1 integrin complex formation is a prerequisite for the endothelial cells to detect the matrix stiffness and tune the cell contractility in order to differentiate (Gehler *et al.*, 2009).

As discussed in section 2.1, FLN mutations cause defects in tissue morphogenesis. These defects can be attributed to the role of FLN in mechanical sensing. Similarly, in *Drosophila* FLN, Cheerio, that has been identified as a component of the ring canals in nurse cells, the mutations have been shown to disrupt the ring canal assembly and expansion (M. G. Li *et al.*, 1999; Sokol and Cooley, 2003).

Although the full picture of the FLN mechanical signaling is not known yet, some models have been proposed. As discussed in sections 2.2 and 2.3, it is now clear that FLN16-17, 18-19 and 20-21 form three closely interacting tandem domain pairs. In case of FLN18-19 and 20-21, the first β-strand of the even numbered domain is masking the ligand binding site on the CD face of the subsequent odd numbered domain and this forms the basis of the auto-inhibition of ligand binding in FLNs (Lad *et al.*, 2007). Based on the previous steered molecular dynamics (SMD) simulations on titin Ig domains (Gräter, *et al.*, 2005), it was predicted that FLNa18-19 and FLNa20-21 are arranged in a similar topological manner such that under force, the CD face masking

interactions would be disrupted first, thereby exposing the cryptic ligand binding sites, before any unfolding events would occur. In accordance with this, SMD simulations (Pentikäinen and Ylänne, 2009) using the crystal structure of FLNa19-21 and NMR structure of FLNa18-19 showed a sequential unmasking of the integrin binding sites on FLNs where the inter-domain interaction between domains 18 and 19 was disrupted first, followed by the disruption of domains 20-21. Next, Ehrlicher and colleagues (Ehrlicher *et al.*, 2011) showed that there is a difference in the FLN-ligand binding kinetics upon force application. On one hand they observed a clear increase in the β integrin binding to FLNa under stress and on the other, they saw a marked decline in the FLNa-FILGAP binding. Furthermore, single molecule mechanical measurements using optical tweezers (Rognoni *et al.*, 2012) showed that under a force range of 2-5 pN, FLNa20-21 undergoes a change in conformational equilibrium leading to a higher affinity binding of ligands. This force range is similar to that generated by single myosin II motor (Koenderink *et al.*, 2009) and considerably lower than that required for unfolding of single FLN Ig domains (15 pN for FLNa20 and 30 pN for FLNa21) (Rognoni *et al.*, 2012, Chen *et al.*, 2013). It is interesting to note that in *Drosophila,* Cher mutants lacking the C-terminal domains corresponding to FLN domains 18-21, exhibit defective oogenesis phenotype in flies (Sokol and Cooley, 2003).

All of these experiments conform to the role of filamins as transducers of mechanical and biochemical cues. It is clear that the non-contiguous arrangement of domains in FLNs plays a role in regulating ligand binding under physiological force. However, in order to fully understand how filamins exert their function as mechanically sensitive springs, further investigation into the structure of the entire Rod region is required.

3 AIMS OF THE STUDY

In order to test the hypothesis that there are mechanically regulated interaction sites in the N-terminal Rod 1 region of FLNs and that the arrangement of the Rod 2 domains in a *Drosophila* model is similar to that of the mechanosensor Rod 2 region in humans, this thesis has three main aims:

1. To understand the inter-domain organization of the N-terminal Rod 1 region of Filamins
2. To investigate the structure and possible functions of the newly found three domain module of domains 3-5
3. To investigate if the inter-domain organization of *Drosophila melanogaster* Filamin, Cher, is identical to human Filamins in the C-terminal Rod 2 region

4 SUMMARY OF THE METHODS

TABLE 2 Summary of the techniques used in this thesis. Details of the methods are described in the original publications and manuscripts attached at the end of this summary.

Method	Article
Ligation independent cloning	I, II, III
Site directed mutagenesis	I, III
Bacterial protein expression	I, II, III
Protein purification	I, II, III
Small angle x-ray scattering (SAXS) data collection	I, II, III
SAXS data processing	I, II, III
SAXS modeling - *Ab initio* and rigid body	I, II, III
Ensemble optimization method (EOM)	I, II
Crystallization	I
Crystal data collection	I
Crystal structure determination and refinement	I
NMR measurements *	I
ThermoFluor assays	I
Molecular dynamics*	I
Pull-down assays	I

*These techniques were performed by Dr Helena Tossavainen, Dr Perttu Permi (NMR) and Dr Ulla Pentikäinen (MD)

5 RESULTS AND DISCUSSION

5.1 SAXS studies revealed four compact domain-domain interactions in the Rod 1 region of Filamin

At the beginning of this study, there was no direct evidence of any mechanically regulated interactions in the Rod 1 region. Previous investigations had always emphasized on the importance of Rod 2 domains in the mechanosensor role of filamins. On the other hand, there are several interaction partners (Zhou *et al.*, 2010) and human point mutations in Rod 1 as well (Bicknell *et al.*, 2007; Krakow *et al.*, 2004; Kyndt *et al.*, 2007; Robertson *et al.*, 2003; Shatunov *et al.*, 2009). Mutations in the Rod 1 causing OPD (Robertson *et al.*, 2003) and Myofibrillar myopathies (MFM) (Shatunov *et al.*, 2009) show clinical symptoms of short stature, bowed bones and abnormal digits, and muscle weakness that could be attributed to loss of mechanosensing function of FLNs.

In addition to the human patient mutations, there are other interesting features of the FLN Rod 1 region as well. For example, the first indications of a second actin binding site in the domains 9-15 came from the structural studies conducted by Nakamura *et al.* (Nakamura *et al.*, 2007). Ithychanda and colleagues (Ithychanda *et al.*, 2009) then characterized domains 4, 9 and 12 to be highly similar to the other ligand-binding domains of FLN and showed binding of GPIbα peptide to these domains. On the same lines, Djinovic-Carugo and colleagues (Djinovic-Carugo and Carugo, 2010) computed the isoelectric potentials (pI) of the Rod domains and showed a regular pattern of alternating pIs of neighboring domains in FLNa, b and c. This correlates with the existence of three domain pairs in the Rod 2 region of FLNa: domains 16-17, 18-19 and 20-21. Furthermore, sequence comparisons of different FLNs showed a repeating pattern of tandem two domain duplications (Light *et al.*, 2012). In this study, domains 4, 9 and 12 were highlighted as being highly identical to the pair forming domains 19 and 21.

In order to obtain direct structural evidence of whether there are any domain-domain interactions in the Rod 1 region of FLNs, we studied all

possible two-domain fragments from this region of FLNc using SAXS. Altogether, 14 two-domain constructs were cloned, expressed and purified. First, the experimental scattering curves of three constructs, FLNc domains 3-4, 4-5 and 14-15, showed globular features in the low angle range (I, Figure 1) suggesting that they exhibit different solution behavior as compared to the rest of the constructs (I, Figure 1). Next, the SAXS derived size related parameters were calculated for all constructs (I, Table I) and the average R_g (mean square distances from the centre of mass weighted by electron densities) and D_{max} (maximum dimension of the particle) turned out to be 2.29 nm and 7.65 nm, respectively. Interestingly, here four constructs were designated as being compact, domains 3-4, 4-5, 11-12 and 14-15, on the basis of them having smaller than the average R_g and D_{max}.

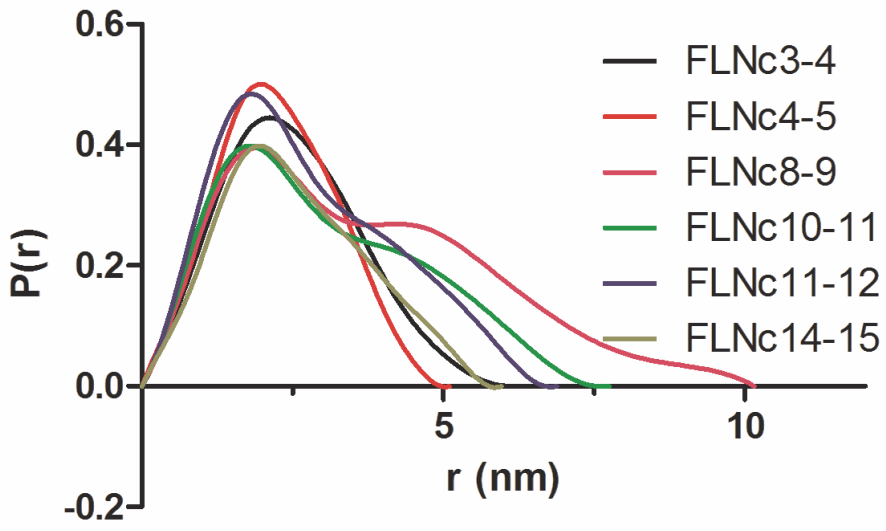

FIGURE 9 Distance distribution profile of the four compact fragments vs. Domains 8-9 (most extended) and domains 10-11 (with average D_{max}).

In addition, their values were in the same range as for the domain pairs in the Rod 2 region (Heikkinen *et al.*, 2009). In the distance distribution plot, domains 3-4 and 4-5 displayed a compact gaussian profile and although domains 11-12 and 14-15 have a smaller than average D_{max}, they showed bimodal peaks. These observations suggest that domains 3-4 and 4-5 are globular while 11-12 and 14-15 exhibit some degree of flexibility (Figure 9). This is in accordance with the dimensionless Kratky plot analysis that showed domains 4-5 to be least and domains 11-12 to be most flexible (I, Figure 2 B) among the four compact domain pairs.

Furthermore, we generated two types of models for each construct, *ab-initio* (envelopes) and rigid body, based on the D_{max} and hydrated particle volume, and experimental scattering data, respectively, to visualize the shape of

the domains in solution. The two models superimposed on each other with good quality indicators. The compactness and globularity (Figure 10) of the models of the putative domain pairs was in the order of, domains 4-5 being the most compact, followed by 14-15 and 3-4. The shape profile for the models of domains 11-12 was similar to that of the extended two-domain constructs with average D_{max} (domains 10-11). The rigid body models in particular suggested that domains 4-5 interact with each other side-by-side as opposed to domains 3-4, 11-12, and 14-15, where one domain seems to be tilted with respect to the other. The models for the rest of the two domain (I, Supporting information S5) constructs suggested them being elongated where two domains interact only at their ends.

To summarize, in our SAXS screening, we have obtained structural evidence that shows existence of four inter-domain interactions in the Rod 1 region of FLNc. Earlier studies (Ithychanda at al., 2009; Light *et al.*, 2012) had predicted that domains 4, 9 and 12 might be involved in inter-domain interactions, however, in our experiments, we only noticed interactions involving domains 4 and maybe 12 but not domain 9. And even though the hydrodynamic parameters obtained from SAXS (D_{max} and R_g) suggest domains 11-12 to be compact, further data analysis and modeling shows these domains to be at the borderline between being compact and fully extended. Domains 3-4, 4-5 and 14-15 are therefore clearly the new candidates with potential domain-domain interactions brought forward as a result of this study.

Interestingly, these interactions were not observed in the electron microscopic (EM) studies (Nakamura *et al.*, 2007). A possible explanation for that may be that whilst the domain pairs in the Rod 2 region are consecutive and form a six-domain compact arrangement, the inter-domain interactions in the Rod 1 are interspersed with extended regions. In that case, the resolution of EM may be a limiting factor for detecting these regions in Rod 1.

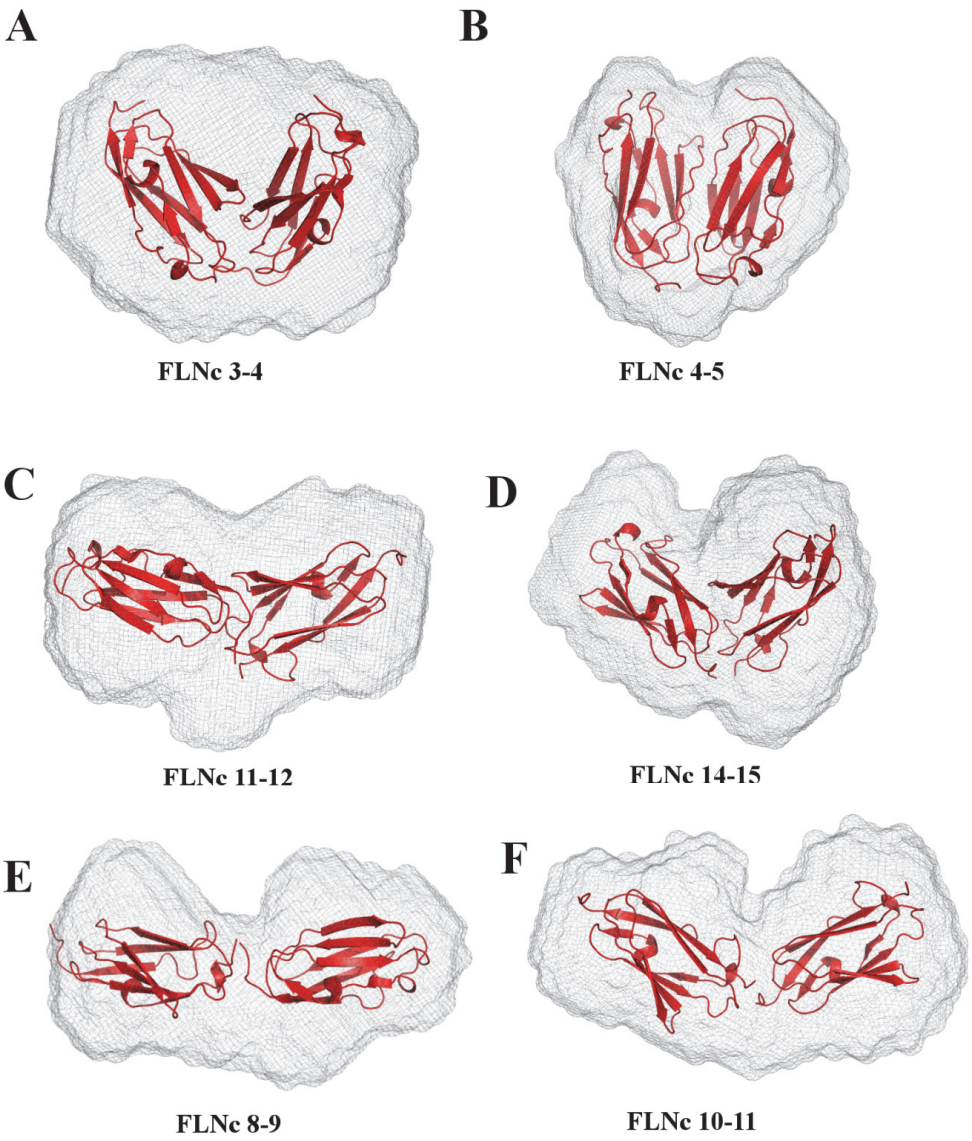

FIGURE 10 Ab-initio envelopes (gray) and rigid body models (red cartoons) of selected two-domain constructs are superimposed. The order of most compact to least compact fragments is: domains 4-5 (B), 14-15 (D), and 3-4 (A); domains 11-12 are intermediate (C). Domains 8-9 are the most extended two-domain fragment (E) and domains 10-11 are the average two-domain fragment (F).

5.2 First report of the crystal structures of FLNa domain 3, FLNa and FLNc domain 4 and 5

Before these studies, there were 8 NMR and 2 crystal structures available in the PDB for the individual domains from the Rod 1 region of FLNs. Amongst them, majority of the NMR structures were for FLNb (domains 9 (PDB ID: 2DI9), 10 (PDB ID: 2DIA), 11 (PDB ID: 2DIB), 12 (PDB ID: 2DIC), 13 (PDB ID: 2DJ4), 14 (PDB ID: 2E9J), 15 (PDB ID: 2DMB)) and for FLNc14 (PDB ID: 2D7M). The two crystal structures were that of FLNa10 (PDB ID: 3RGH) (Page *et al.*, 2011) and FLNb1 (PDB ID: 4B7L) (Sawyer *et al.*, 2012).

In our attempt to achieve high-resolution structures of the four compact regions that we discovered in the SAXS screening, I was able to obtain crystal structure of FLNc4-5 and subsequently, Jonne Seppälä solved the structure of FLNa3-5. In this section, I analyze the structures of all these individual domains, i.e. FLNa3, FLNa4, FLNc4, FLNa5 and FLNc5.

All the domains have a typical Ig domain fold with seven β-strands and the GPG motif in the A strand preceding the 3_{10} helix, except FLNa3 which has GRG in the same position. However, there are subtle differences in the conformations of the β-strands C and D.

In FLNa3, FLNa5 and FLNc5, the loop between the strands C and D is in an outward extended closed conformation (Figure 11, A, D, E, highlighted with an arrow). In FLNa3, the bend in the CD loop is introduced due to the Gly 521 and Pro 522. In case of FLNa5 and FLNc5, the positioning of Pro 718 and Pro 713, respectively, at the beginning of the D strand, contributes to this conformation. This extension may have been further stabilized by a salt bridge between a conserved Asp (713 in FLNa5 and 708 in FLNc5) and Lys (739 in FLNa5 and 734 in FLNc5).

FLNa4 and FLNc4 (Figure 11 B, C), however, do not have this closed conformation of the CD loop. FLNc4, but not FLNa4, has a 3_{10} helix (Figure 11 C, highlighted with an arrow) in the beginning of strand C, formed by three residues 601-603. It is interesting to note that although FLNa4 also has the same amino acid sequence at the corresponding position (606-608), this 3_{10} helix is not seen. One reason for this conformation may be a possible hydrogen bond between Thr 599 and Thr 603 in FLNc4.

When superimposed with the available single domain structures of predicted ligand binding domains (FLNb9, FLNb12, FLNb17, FLNb19, FLNb21), FLNa4 and FLNc4 show a similar conformation at the CD face, except the 3_{10} helix of FLNc4 (Figure 11 F).

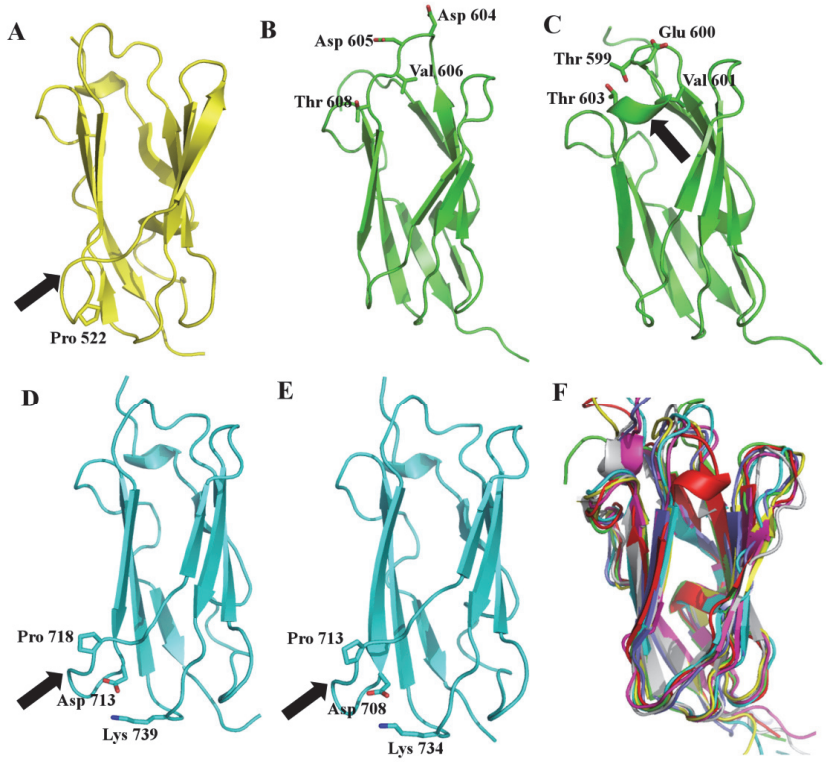

FIGURE 11 Structures of individual FLN domains. **(A)** FLNa3, **(B)** FLNa4, **(C)** FLNc4, **(D)** FLNa5, and **(E)** FLNc5. The residues that are responsible for the special features at the CD face of these domains are labeled. In panels A, D and E, arrows indicate the extension in the CD loop. In panel C, the arrow indicates the 3_{10} helix in the beginning of strand C. **(F)** Superposition of the known available single domain structures of predicted ligand binding domains (FLNb9- pink, FLNb12- yellow, FLNb17- cyan, FLNb19- blue, and FLNb21- gray) with FLNa4- green and FLNc4- red.

5.3 Crystal structures of FLN domains 3-5 show a new type of interactions between Immunoglobulin-like domains

The crystal structure determination of FLNc4-5 and FLNa3-5 was performed to find out details of the interactions between the domains. These structures revealed new type of interfaces between FLN domains. Instead of interacting along the edges of the β sheets (as seen in FLNa16-17, 18-19, 20-21 and FLN domain 24 dimer, see section 2.3 above), domains stack side-by-side along their β sheets forming a sandwich (Figure 12 A). In this sandwich, the β sheets of the

domains are roughly stacked on top of each other in parallel, except domain 3, which is slightly shifted. Here, the interaction between domains 3 and 4 is mostly mediated by polar residues at the edges of the β sheets, i.e involving residues at the A strand of domain 3 and at the F and G strands of domain 4. On the other hand, the interaction between domains 4 and 5 is mediated by three β-strands from each domain, where the highest contribution is of the large hydrophobic surface around a Trp residue in the A strand of domain 4 (Trp 582 in FLNa and Trp 577 in FLNc) (II, Figure 2 B, C). The overall arrangement of domains 4 and 5 in FLNa is almost identical to FLNc4-5 with a root mean square standard deviation (rmsd) of 0.66 Å between 165 C-α atoms. The buried interface area between domains 4-5 is larger (830 Å^2) than between domains 3-4 (500 Å2) suggesting that the interaction between domains 4-5 is tighter than domains 3-4.

The kind of domain-domain interface that is seen in FLN 4-5 is also novel with respect to the Immunoglobulin domain superfamily itself. In antibodies, for instance, typical immunoglobulin-immunoglobulin domain interactions are mediated either along the face of the β sheets from two domains or along the edges of the β sheets from the two domains, but always in perpendicular orientation (Biersmith *et al.*, 2011; Müller *et al.*, 2013; Wurzburg and Jardetzky, 2009) (Figure 12 B).

As these structures are unique, we used several complementary techniques to validate the existence of the domain-domain interactions in solution. The first check we conducted was to back calculate the scattering from the crystal structures of FLNa3-5 and FLNc4-5 and fit it with the experimental SAXS scattering of these constructs. The goodness of the fits, which is determined by the chi values (the lower the value, the better the fit), was 1.13 and 1.80 for FLNa3-5 and FLNc4-5, respectively. Next, we superimposed the crystal structures in the SAXS-generated *ab-initio* envelopes and obtained good fits (Normalized Spatial Discrepancy (NSD) for FLNc4-5 was 2.41 and for FLNa3-5 was 1.63) (II, Figure 2 D, E). To check for conformational changes upon mutations of the interacting residues at the interface of domains 4 and 5, we made a combination of single and double mutations on the two-domain fragment of FLNc4-5 and screened them with SAXS. All the mutants showed a noticeable change in the D_{max} and R_g parameters (II, Table 2), suggesting that the mutations loosened the tight packing between the two domains. The same mutations also abolished the interaction between single domains of FLNc4 and FLNc5 in pull down assays (II, Figure 4A and B). Finally, Drs Helena Tossavainen and Perttu Permi conducted NMR measurements to compare the ^{1}H- ^{15}N HSQC spectra of FLNc5 against FLNc4-5 (II, Figure 4 C, D and Figure S2) and observed chemical shifts of more than 0.25 ppm for the residues at the β-strands CFG of domain 5, which are the interacting with domain 4 in the crystal structure. All these experiments coherently confirm that the interface between FLN domains 4-5 in the crystal structure is the same as in solution.

To gain some insight into the flexibility of domain 3, on the account of it occupying a comparatively small interaction area with domain 4, we performed

ensemble optimization method (EOM) analysis on the SAXS data of FLNa3-5, FLNc3-5 and FLNc4-5 (II, Figure 5 A, B). The R_g and the D_{max} range obtained for the selected models of FLNc4-5 showed a narrow distribution suggesting that it is mostly compact. On the contrary, we noticed a bimodular peak distribution of R_g and the D_{max} for the selected models of FLNa and FLNc3-5 suggesting them to be flexible, i.e domain 3 being the flexible component. This conclusion was buttressed by molecular dynamics (MD) simulations with FLNa3-5 crystal structure performed by Dr Ulla Pentikäinen. Over a duration of 50 nanoseconds, domain 3 oscillated between two extreme orientations with respect to intact domains 4- 5 (II, Figure 5 C).

To summarize, the crystal structures solved in this study have disclosed a new type of Ig-domain packing where the interacting residues are conserved throughout the animal kingdom (II, Figure 3) suggesting that this arrangement of domains 3-5 may be a common feature in FLNs.

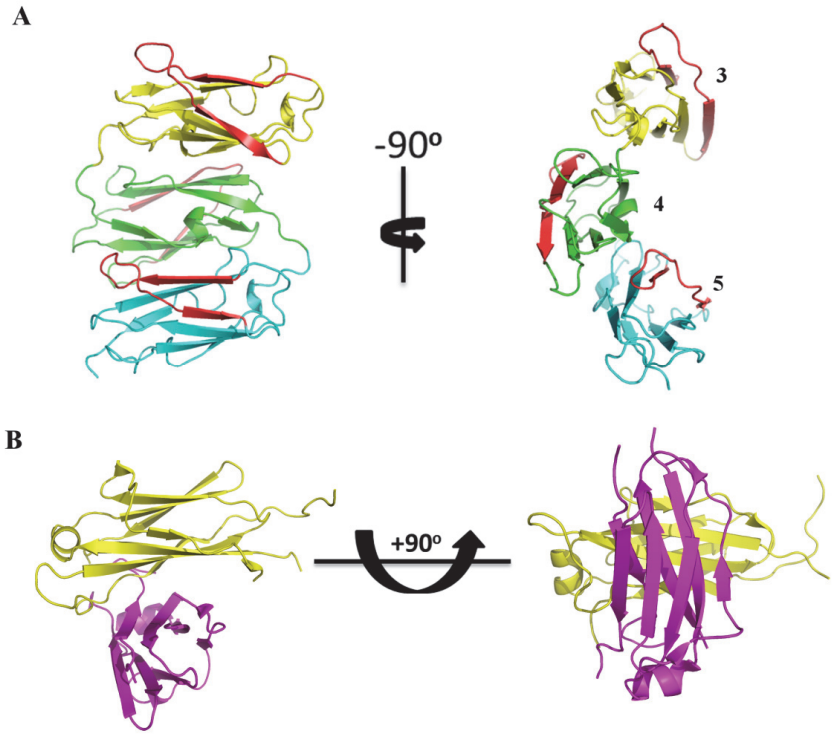

FIGURE 12 Immunoglobulin domains interactions. (A) Crystal structure of FLNa3-5 showing the stacking arrangement of the three domains. The CD faces of each domain are shown in red. (Reproduced with permission from © the American Society for Biochemistry and Molecular Biology) (B) Crystal structure (PDB ID: 4JVU) of Immunoglobulin M Fc domains. Each domain of the dimer is shown in a different color. Note the perpendicular arrangement of the domains.

5.4 Domain 4 is able to bind a typical β-strand containing ligand peptide

To gain insight into the function of the novel three-domain module, we next focused our attention on the interaction of this fragment with the β-strand forming peptides. As discussed above, these peptides typically bind the CD face of FLN domains by forming a new strand next to the strand C. In our structures, the CD faces of all the three domains were exposed to the solvent (Figure 12 A). However, the CD faces of all the domains under investigation, except FLNa4, were in a conformation that seemed unlikely for a ligand to bind to (Figure 11).

In order to test if FLNc domain 4 would still bind a ligand, in spite of the 3_{10} helix at the beginning of the strand C at the putative ligand binding site, I co-crystallized FLNc4-5 with a peptide derived from the GPIbα cytoplasmic tail (residues 573-596, RGSLPTFRSSLFLWVRPNGRVGPL), that is known to have the highest affinity amongst the known FLN binding ligands (Ithychanda *et al.*,2009a). The structure (Figure 13) showed that the peptide does interact with FLNc4 by forming an anti-parallel β-strand next to the strand C at the CD face by using the previously characterized β-sheet augmentation mechanism. The nine residues of the peptide (PTFRSSLFL) form main chain hydrogen bonds with the strand C of domain 4 and interact with the hydrophobic side chains of strand D in a similar way as seen with the same peptide and FLNa17 earlier (Nakamura *et al.*, 2006) (Table I , and II, Figure 6F). Interestingly, in the ligated structure, the electron density was not seen for the residues forming the 3_{10} helix in the unligated structure. This suggests that this part is flexible and has been accommodated upon peptide binding. Likewise, the BC loop of FLNc4 was not visible here, suggesting local flexibility in the ligated structure.

The peptide interaction studies were validated and extended for FLNa by NMR. ^{15}N- and ^{13}C-HSQC spectra of FLNa3-5 and ^{15}N-HSQC spectra of FLNc4-5 were collected in the presence and absence of the GPIb peptide. In both isoforms, the chemical shift changes were observed at or close to the CD face of domain 4 (II, Figure 6G, H and Figure S3). Interestingly, two sets of cross peaks were observed in the spectra for the residues of the 3_{10} helix in domain 4 of FLNc4-5 fragment in the absence of the peptide (Tossavainen *et al.*, 2014). On the other hand, only a single set of peaks is observed for the same residues in the spectra of FLNa3-5 which doesn't have the 3_{10} helix. This suggests that helix is flexible in FLNc4 in the absence of the peptide.

To summarize, our results have confirmed that the novel domain -domain interactions in FLNa3-5 and FLNc4-5 do not interfere with the binding of a small β-strand forming peptide to domain 4 and also that the CD face of FLNc4 is available for binding to the peptide and the 3_{10} helix at the beginning of strand C does not interfere with this interaction.

Although Ithychanda and colleagues (Ithychanda, Hsu, *et al.*, 2009) had shown previously using NMR and ITC that FLNa4 binds to GPIbα peptide, this

is the first time that a high resolution structure has been solved showing the structural details of the interaction.

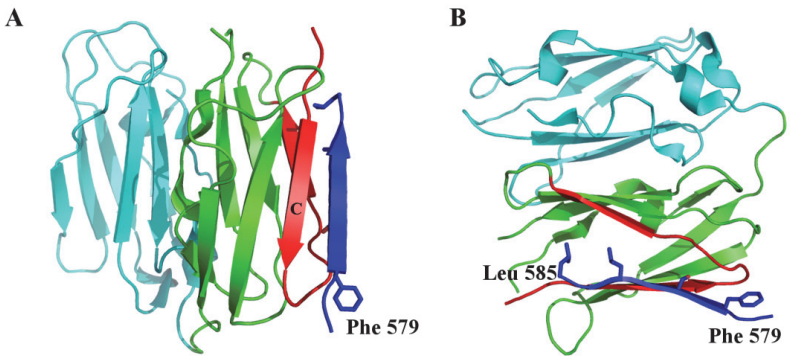

FIGURE 13 Crystal structure of FLNc4-5 with GPIbα peptide. FLNc4 is shown in green and FLNc5 in cyan. The peptide is shown in blue. The CD face of domain 4 is shown in red. (A) The anti-parallel orientation of the peptide with the strand C of domain 4 is shown. (B) This panel shows the location of the interacting residues of the peptide and the orientations of their side chains.

5.5 Domain 5 stabilizes the structure of domain 4 and positively regulates the ligand interaction with domain 4

Previous peptide binding studies using NMR and ITC measurements had shown FLNa4 to be partially unstable (Ithychanda, Hsu, *et al.*, 2009). In our hands, FLNa3-5 and FLNc4-5 behaved well for the GPIbα peptide binding experiments using NMR.

In order to test if the neighboring domains have an effect on the stability of domain 4, we performed thermal melting assays (Thermofluor) using a hydrophobic fluorescent dye (Figure 14). Temperature dependent dye binding curve of single domain FLNc4 showed that the dye starts binding around 35-45 ˚C. On the other hand, the curve of FLNc5 showed the dye to bind in the range of 70-80 ˚C. This suggests that FLNc4 is less stable than FLNc5. Next, the same experiment using FLNc4-5 showed two peaks where the first peak starts appearing around 55 ˚C and the second one around 70 ˚C. This indicates that domain 5 stabilizes the structure of domain 4. This can be explained by the large hydrophobic surface that is exposed to the solvent in domain 4 but is buried in the presence of domain 5. On the other hand, the thermal melting curve of the three-domain fragment of FLNc3-5 looked similar to that of FLNc4-5, suggesting that domain 3 does not have any additional effect on the stability of domain 4.

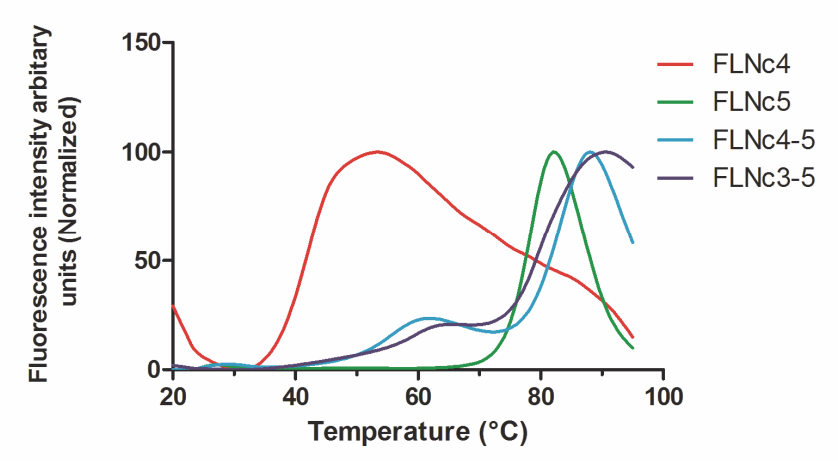

FIGURE 14 Thermal stability of FLNc4, 5, 4-5 and 3-5. Thermal melting curves of FLNc4 (red), FLNc5 (green), FLNc4-5 (cyan) and FLNc3-5 (blue) are shown. (Reproduced with permission from © the American Society for Biochemistry and Molecular Biology)

5.6 Rod 2 domains in Cher have similar inter-domain interactions as in Filamins

Filamins have been shown to play a role in cell differentiation and tissue morphogenesis (Zhou *et al.*, 2010). As discussed in section 2.4, the three tandem domain pairs in the Rod 2 region of FLNs have been implicated to act as mechanosensor modules that tune the cell morphology.

In order to gain a direct evidence of the mechanosensor role of FLNs in cell differentiation, *Drosophila melanogaster* isoform of FLN protein, Cher, serves as a good model for the following reasons: a) Even though Cher has 20 Ig domains as compared to 24 in vertebrates, sequence alignments have shown that the Rod 2 region of Cher has a domain arrangement similar to that of vertebrate FLNs (Heikkinen *et al.*, 2009), b) Cher Ig domains share 34-52% sequence similarity with human FLNs (Van der Flier and Sonnenberg, 2001) where the A strands of Cher domains 14 and 16 look similar to FLN domains 18 and 20 (III, Figure 1), and c) Rod 2 truncated mutants of Cher show inability to recruit actin filaments which causes ring canal defects leading to impaired oogenesis (Sokol and Cooley, 2003).

However, prior to conducting any experiments in-vivo, we tested behavior of the Cher constructs in solution to gain information on the stability and hydrodynamic parameters of the five-domain fragment of Cher consisting of domains 13-17 that are orthologous to FLN domains 17-21. To this end, we have targeted mutations to the first β-strand of domains 14 and 16. One mutant was made such that it would form an open mechanosensor, by substituting Ile

with Glu in the A strand of domains 14 and 16 to disrupt their interaction with domains 15 and 17, respectively. We refer to this mutant as Cher-Astr. The second mutation was made such that it would form a closed mechanosensor, by substituting some of the key interacting residues at the A strand of domains 14 and 16 with the FLN domain binding motif of GPIbα peptide. We refer to this mutant as Cher-GP. The mutated residues are highlighted in article III, Figure 1.

The wild type construct and the two mutants were successfully expressed and purified. Small differences in the elution volumes were already observed during purification using size exclusion chromatography (SEC) (III, Figure 2) indicating that Cher-Astr construct had a higher hydrodynamic volume as compared to the wild type Cher (Cher-WT) and Cher-GP.

We further screened these three constructs using SAXS. The experimental scattering profile of Cher-Astr (III, Figure 3 B and C, marked with arrow) looked different in the small angle range, indicating it had a different conformation as compared to the other two constructs. Next, we calculated R_g, hydrated particle volume (Porod's volume) and D_{max} for these constructs (III, Table I). The R_g and Porod's volume for Cher-WT and Cher-GP were in the range of a 4-6 domain fragment (Pentikäinen *et al.*, 2011; Ruskamo *et al.*, 2012), in contrast to Cher-Astr which has a higher R_g and Porod's volume suggesting that it is extended or even a dimer. The distance distribution probability curve (Figure 15) also showed that Cher-WT and Cher-GP were more compact with maximum dimensions of 13 nm and 12 nm, respectively as compared to Cher-Astr that showed an extended curve with D_{max} around 15 nm.

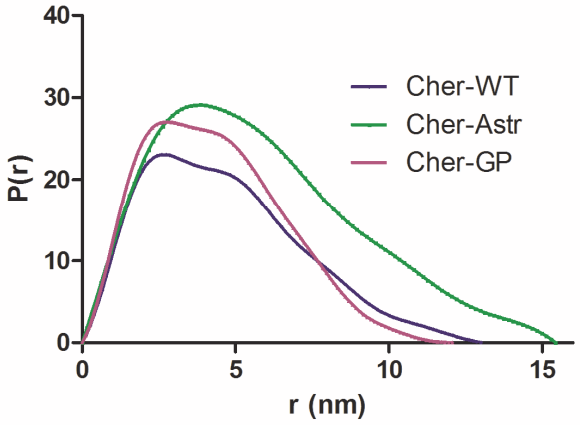

FIGURE 15 Distance distribution probability function plot of Cher-WT, Cher-Astr and Cher-GP constructs

Next, we generated *ab-initio* (III, Figure 5 A, B, D, E, G and H, gray mesh) and rigid body models (III, Figure 5 A, B, D, E, G and H, cartoons) of these constructs to visualize the arrangement of the domains. We applied two

different approaches to generate the rigid body models in order to confirm the existence of the domain pairs. First, we generated models using single domain 23 from FLNc (PDB ID: 2NQC) as a template (III, Figure 5 A, D, G) and checked the fit of these models to the *ab-initio* envelope (NSD) and to the experimental scattering (Chi values shown in III, Figure 5 C, F, I). Then we generated models using FLNa domain pairs 18-19 (PDB ID: 2K7Q) and 20-21 (PDB ID: 2J3S) as templates (III, Figure 5 B, E, H) for Cher domains 14-15 and 16-17, respectively and calculated the fits. Comparison of NSD and Chi values between two types of rigid body models clearly showed that in Cher-Astr construct, the mutations in the A strands of domains 14 and 16 have disrupted their interactions with domains 15 and 17, respectively.

In order to investigate if Cher-Astr construct exists as a dimer in solution, as was indicated by the Porod's volume, we generated another set of rigid body models, but this time, with 10 domains and compared the fit of these models with the model containing 5 domains (III, Figure 6). Interestingly, the fits support the notion of Cher-Astr existing as a dimer in solution.

To summarize, this is the first study investigating the hydrodynamic behavior and structure of the mechanosensor region in Cher. Our results show that Cher wild type fragment of domains 13-17 and the two mutants are stable in solution. We do not observe a big difference in the SAXS behavior of Cher-WT and Cher-GP, which is in line with the assumption that Cher-GP construct is a tight mechanosensor. On the other hand, we clearly see that Cher-Astr construct is extended and the inter-domain interactions are disrupted. However, it is not clear whether it is a dimer or not as on one hand, the SEC elution volumes support the notion of a monomer, but on the other hand, the Porod's volume and the rigid body models support the existence of a dimer.

However, these results, altogether, form a good basis for testing the effect of an open or closed mechanosensor region on the ring canal development during oogenesis in *Drosophila*.

6 CONCLUSIONS

The main conclusions of this thesis are:

1. There are 4 compact regions in the Rod 1 region of filamins. The evidence is stronger for the existence of inter-domain interactions between domains 3-4, 4-5 and 14-15. However, domains 11-12 were on the borderline between interacting and extended domains.

2. FLN domains 3-5 form a compact three-domain module. The inter-domain interactions between these domains revealed a new type of domain -domain packing for the Ig-domain family. The interactions between domains 4 and 5 are tighter than between domains 3 and 4. Domain 4 is able to bind a typical β-strand forming ligand peptide at the CD face using the previously known β sheet augmentation mechanism. Interaction of Domain 5 with domain 4 stabilizes the structure of domain 4, which most likely is a pre-requisite for ligand binding. Taken together, our results and previous studies suggest that in the Rod 1 region, inter-domain interactions, at least in context of domains 3-5, positively regulate ligand binding in contrast to the Rod 2 region, where the domain-domain interactions inhibit binding of the ligand. The finding that GPIbα binds to domain 4 supports the hypothesis of multiple similar ligand binding domains in filamins. It is also interesting to note that despite the fact that platelet tyrosine kinase Syk has been shown to bind to FLNa domain 5 (Falet *et al.*, 2010), in our crystal structures, the CD face of domain 5 is in a conformation that is unfavorable for ligand binding. This suggests that there may be a completely different mechanism by which Syk kinase binds to FLN domain 5.

3. The organization of the mechanosensor region in Rod 2 of Cher is similar to that of human FLNa. The five-domain protein fragment of domains 13-17 along with the two mutants is stable in solution. The mutations designed to open the putative mechanosensitive sites (Cher-Astr) in Cher Rod 2, clearly caused a change in hydrodynamic parameters of the fragment. The mutation designed to

keep the mechanosensor closed (Cher-GP), did not change the hydrodynamic parameters of the fragment.

Acknowledgements

First and foremost, I would like to express my heartfelt gratitude to my mentor and supervisor Professor Jari Ylänne. There are not enough words to explain how much I appreciate you giving me this opportunity to pursue my dream. You have been an excellent guide who has supported me throughout this research and have given me enough space to think and act independently. I have honestly enjoyed every brainstorming meeting with you, even when it has lasted 4 hours.

I would like to thank Adjunct Professor Tassos Papageorgiou and Professor John Trinick for acting as referees for my thesis and providing their valuable feedback within the constraints of a tight deadline.

This work has been primarily funded by the FP7 Marie Curie funding for Initial Training Network- Muscle Z-Disk Protein Complexes (MUZIC). I feel extremely fortunate to have belonged to this network where I had the opportunity to interact and learn from the experts in the field of structural and muscle biology. This network has enriched me not just scientifically but also presented me with new friendships. I thank all the "MUZICians" for the great and fun-filled times in distant countries.

I have been fortunate enough to work with great colleagues. Salla, Heikki, Jonne, Niina, Mikko, Jarkko and Sanna - I am fully aware of how talkative I am and I totally appreciate you guys for listening to me, especially on those chaotic days. I would also like to thank Ulla for her contribution in the JBC paper. I want to express my gratitude to "Allu" for her ever-so-helpful nature. It still amazes me that how we both have managed to communicate perfectly over these years with our english-finnish language issues. I guess "Ei Ongelma" is an important phrase to learn in order to survive in the lab.

Next, I want to thank my finnish family- Leona, Jukka, Malla, Julli, Nadine, Moona, Leena, Kai, Maria, Laura and Marie. I do not even know how to begin expressing my gratitude to you all. You all have been my home away from home. You have brought me breakfast at night when I was writing my thesis, invited me home to eat dinners and overall made sure I was alive during the thesis writing process. I will always remember and cherish this memory of working with friends and laughing in the corridor for no reason whatsoever. And it goes without saying that I totally appreciate you "tolerating" my craziness and hyper behavior. You guys deserve a medal.

I am blessed to have friends like Pallavi, Nisha and Deepti. Our friendship is a proof that distance does not matter. You all have been there for me with your soothing words whenever I was in need of support and with your crazy hats when I was in need of letting my hair down.

Last but not the least; I want to thank my parents for their support through thick and thin. You have been my rock who has kept me grounded and taught me to be humble and modest in whatever I do. I always found it amazing that even though you did not understand my research so well, you have always been curious and offered me valuable advice in dire circumstances.

This PhD would not have been possible without your constant support and motivation.

YHTEENVETO (RÉSUMÉ IN FINNISH)

Filamiini-proteiinien domeenien väliset vuorovaikutukset

Väitöskirjatyöni käsittelee ensisijaisesti proteiinirakenteita. Tutkimukseni kohteena on proteiiniperhe nimeltään filamiinit. Filamiinien tehtävänä solussa on liittää solunsisäisiä aktiinisäikeitä yhteen ja toimia sitoutumispaikkana näihin säikeisiin liittyville solukalvon proteiineille sekä erilaisille solunsisäisille viestinvälittäjäproteiineille. Mielenkiintoiseksi filamiinien rakenteiden tutkimisen tekevät uudet tutkimustulokset siitä, että aktiinisäikeisiin kohdistuva vetovoima voi lisätä tai vähentää filamiinien sitoutumista toisiin proteiineihin. Ilmeistä on, että filamiinit osallistuvat solujen ja kudosten mekaanisten ominaisuuksien säätelyyn, mikä on tärkeää kudosten muodon ja koon määräytymisessä. Tutkimusryhmämme oli aikaisemmin selvittänyt, miten tämä mekaaninen säätely toimii rakennetasolla filamiini A:n kahdessa sitoutumiskohdassa, immunoglobuliinin kaltaisissa domeeneissa 19 ja 21. Näissä kohdissa sitoutumispaikka on normaalisti peittynyt edellisen domeenin toimesta ja tämä peittyminen vapautuu filamiinia venytettäessä.

Väitöskirjani kahden ensimmäisen osatutkimuksen tavoitteena oli selvittää, onko filamiiniproteiinien muissa osissa samantapaisia mekaanisesti säädeltyjä sitoutumispaikkoja kuin domeeneissa 19 ja 21. Lähtöhypoteesiksi otettiin, että tällaisissa mekaanisesti säädellyissä sitoutumispaikoissa kahden peräkkäisen proteiinidomeenin välillä on tiiviimpi vuorovaikutus kuin muualla. Tutkimuksen ensimmäisessä osassa tuotin ja puhdistin kaikki mahdolliset peräkkäisten kahden domeenin palat ihmisen filamiini C:n domeeneista 1-15. Näitä analysoin röntgensirontatekniikoilla liuostilassa Saksan elektronisynkrotronilaitoksella (DESY, Deutche Electronensynchroton) Hampurissa ja Euroopan synkrotronisäteilytyslaitoksella (ESRF, Europan Synchrotron Radiation Facility) Grenoblessa, Ranskassa. Sirontatulosten analysointi erilaisilla laskennallisilla tekniikoilla ja mallintamalla osoitti, että neljä näistä kahden domeenin palasta oli tiiviimmin pakkautuneita kuin muut kymmenen. Näiden kokeellisesti löydettyjen uusien domeenien välisten vuorovaikutuspaikkojen sijainti filamiinissa on eri kuin mitä aikaisemmin oli ennustettu proteiinisekvenssivertailujen perusteella. Mielenkiintoista oli etenkin se, että domeenit 3, 4 ja 5 voisivat näiden tulosten perusteella muodostaa kolmen domeenin tiiviisti pakkautuneen alueen.

Seuraavaksi keskityttiin filamiinin domeenien 3-5 muodostaman alueen tarkempaan analyysiin. Tässä käytettiin liuostilan röntgensironnan lisäksi myös proteiinikristallografiaa. Kiteiden sirontamittauksia tehtiin jälleen synkrotroneilla, koska proteiinikiteet olivat pieniä ja suhteellisen huonosti siroavia. Oma kokeellinen työni keskittyi etenkin filamiini C:n domeeniparin 4-5 atomitason rakenteeseen yksinään ja sitoutuneena verihiutaleiden kalvoproteiinin solunsisäiseen osaan. Lisäksi väitöskirjassani käsitellään yhteistyössä Jonne Seppälän kanssa analysoitua filamiinin A:n domeenien 3-5 rakennetta. Tuloksemme osoittivat, että domeenien 4 ja 5 vuorovaikutuspinta on filamiineissa suhteelli-

sen suuri ja näin ollen vuorovaikutus on voimakas verrattuna aikaisemmin julkaistuihin filamiinien domeenien välisiin vuorovaikutuksiin. Osoitimme, että tällä alueella domeeni 4 on tärkeä verihiutaleiden sitoutumispaikka ja domeeni 5 stabiloi domeeni 4:n rakennetta. Kiderakenteessa havaitut domeenien väliset vuorovaikutukset ja kalvoproteiinin sitoutumispaikka varmennettiin mutaatiokokeilla, biokemiallisilla kokeilla ja käyttäen ydinmagneettista resonanssispektroskopiaa (NMR). Kokonaisuudessaan nämä rakennetutkimukset osoittavat, että filamiinien domeenien 3-5 välinen pakkautumien on aivan erilainen kuin aikaisemmin oli löydetty domeenien 19 ja 21 lähellä. Tämä uusi pakkautumistapa ei johda domeenin 4 sitoutumispaikan peittymiseen. On kuitenkin mahdollista, että mekaaninen veto irrottaa domeenit 4 ja 5 toisistaan, mikä muuttaa domeenin 4 epävakaaksi ja vähentää sen sitoutumiskykyä.

Väitöskirjani kolmannessa osatutkimuksessa selvitimme *Drosophila melanogaster* banaanikärpäsen filamiinin rakennetta. Erityisesti keskityimme ihmisen filamiinin domeeneja 19 ja 21 vastaavaan osaan. Tavoitteena oli varmistaa, että pistemutaatiot, joiden tarkoitus on muuttaa banaanikärpäsen filamiinin mekaanisia ominaisuuksia, todella muuttavat proteiinin rakennetta suunnitellulla tavalla. Tutkimuksessa osoitin, että suunnitellut mutaatiot eivät muuta yhdistelmä-DNA -tekniikoilla tuotettujen proteiinipalojen stabiilisuutta. Osoitin myös, että mutaatio, jonka oli suunniteltu vähentävän domeenien välistä vuorovaikutusta, teki proteiinipalasta huomattavasti joustavamman kuin vastaava alkuperäinen proteiini. Tämä luo hyvän pohjan näiden mutaatioiden käyttämiselle filamiinin mekaanisen säätelyn tutkimiseen banaanikärpäsen kudosten kehityksessä.

Kokonaisuudessaan tämä tutkimus on tuottanut uutta tietoa filamiinien rakenteesta ja vuorovaikutuksista. Pitkällä tähtäimellä toivon tämän tiedon auttavan filamiinien toiminnan ymmärtämisessä ja sen selittämisessä, miksi jotkut ihmisten filamiinien perinnölliset mutaatiot aiheuttavat kehityshäiriöitä ja kudosten epämuodostumia.

REFERENCES

Bañuelos, S., Saraste, M., and Djinović Carugo, K. 1998. Structural comparisons of calponin homology domains: implications for actin binding. *Structure* 6: 1419–1431.

Bicknell, L.S., Farrington-Rock, C., Shafeghati, Y., Rump, P., Alanay, Y., Alembik, Y., Al-Madani, N., Firth, H., Karimi-Nejad, M.H., Kim, C.A., Leask, K.., Maisenbacher, M., Moran, E., Pappas, J.G., Prontera, P., de Ravel,T., Fryns, J.P., Sweeney, E., Fryer, A., Unger, S., Wilson, L.C., Lachman, R.S., Rimoin, D.L., Cohn, D.H., Krakow, D., and Robertson, S.P. 2007. A molecular and clinical study of Larsen syndrome caused by mutations in FLNB. *J. Med. Genet.* 44: 89–98.

Biersmith, B. H., Hammel, M., Geisbrecht, E. R., and Bouyain, S. 2011. The immunoglobulin-like domains 1 and 2 of the protein tyrosine phosphatase LAR adopt an unusual horseshoe-like conformation. *J. Mol. Biol.* 408: 616–627.

Bresnick, A. R., Janmey, P. A., and Condeelis, J. 1991. Evidence that a 27-residue sequence is the actin-binding site of ABP-120. J. Biol Chem.266: 12989–12993.

Brotschi, E. A., Hartwig, J. H., and Stossel, T. P. 1978. The gelation of actin by actin-binding protein. *J. Biol Chem.* 253: 8988–8993.

Calderwood, D.A., Huttenlocher, A., Kiosses,W.B., Rose, D.M., Woodside, D.G., Schwartz, M.A., and Ginsberg, M.H. 2001. Increased filamin binding to β -integrin cytoplasmic domains inhibits cell migration. *Nat. Cell. Biol.* 3: 1060-1068.

Chen, H., Chandrasekar, S., Sheetz, M. P., Stossel, T. P., Nakamura, F., and Yan, J. 2013. Mechanical perturbation of filamin A immunoglobulin repeats 20-21 reveals potential non-equilibrium mechanochemical partner binding function. *Sci. Rep.* 3: 1642.

D'Addario, M., Arora, P. D., Fan, J., Ganss, B., Ellen, R. P., and McCulloch, C. A. 2001. Cytoprotection against mechanical forces delivered through beta 1 integrins requires induction of filamin A. *J. Biol. Chem.* 276: 31969–31977.

Dalkilic, I., Schienda, J., Thompson, T. G., and Kunkel, L. M. 2006. Loss of FilaminC (FLNc) results in severe defects in myogenesis and myotube structure. *Mol. Cell. Biol.* 26: 6522–6534.

Djinovic-Carugo, K., and Carugo, O. 2010. Structural portrait of filamin interaction mechanisms. *Curr. Protein Pept. Sci.* 11: 639–650.

Ehrlicher, A. J., Nakamura, F., Hartwig, J.H., Weitz, D.A, and Stossel, T.P. 2011. Mechanical strain in actin networks regulates FilGAP and integrin binding to filamin A. *Nature* 478: 260–263.

Falet, H., Pollitt, A.Y., Begonja, A.J., Weber, S.E., Duerschmied, D., Wagner, D.D., Watson, S.P., and Hartwig, J.H. 2010. A novel interaction between FlnA and Syk regulates platelet ITAM-mediated receptor signaling and function. *J. Exp. Med.* 207: 1967–1979.

Farrington-Rock, C., Kirilova, V., Dillard-Telm, L., Borowsky, A.D., Chalk, S., Rock, M.J., Cohn, D.H., and Krakow, D. 2008. Disruption of the Flnb gene in mice phenocopies the human disease spondylocarpotarsal synostosis syndrome. *Hum. Mol. Genet.* 17: 631–641.

Feng, S., Reséndiz, J. C., Lu, X., and Kroll, M. H. 2003. Filamin A binding to the cytoplasmic tail of glycoprotein Ibalpha regulates von Willebrand factor-induced platelet activation. *Blood* 102: 2122–2129.

Feng, Y., Chen, M. H., Moskowitz, I. P., Mendonza, A. M., Vidali, L., Nakamura, F., Kwiatkowski, D.J., and Walsh, C. A. 2006. Filamin A (FLNA) is required for cell-cell contact in vascular development and cardiac morphogenesis. *Proc .Natl. Acad. Sci. U S A.* 103: 19836–19841.

Flier, A. Van Der, and Sonnenberg, A. 2001. Structural and functional aspects of filamins. *Biochim. Biophys. Acta* 1538: 99-117.

Fürst, D.O., Goldfarb, L.G., Kley, R. A, Vorgerd, M., Olivé, M., and Van der Ven, P.F.M. 2012. Filamin C-related myopathies: pathology and mechanisms. *Acta Neuropathol.* 125: 33-46.

Gadsby, D. C., Vergani, P., and Csanády, L. 2006. The ABC protein turned chloride channel whose failure causes cystic fibrosis. *Nature* 440: 477–483.

Gardel, M. L., Schneider, I. C., Aratyn-Schaus, Y., and Waterman, C. M. 2010. Mechanical integration of actin and adhesion dynamics in cell migration. *Annu. Rev. Cell Dev. Biol.* 26: 315–333.

Gehler, S., Baldassarre, M., Lad, Y., Leight, J. L., Wozniak, M. A., Riching, K. M., Eliceiri, K.W., Weaver, V.M., Calderwood, D.A., and Keely, P. J. 2009. Filamin A-beta1 integrin complex tunes epithelial cell response to matrix tension. *Mol. Biol. Cell.* 20: 3224–3238.

Glogauer, M., Arora, P., Chou, D., Janmey, P. A, Downey, G. P., and McCulloch, C. A. 1998. The role of actin-binding protein 280 in integrin-dependent mechanoprotection. *J. Biol Chem.* 273: 1689–1698.

Glogauer, M., Arora, P., Yao, G., Sokholov, I., Ferrier, J., and McCulloch, C. A. 1997. Calcium ions and tyrosine phosphorylation interact coordinately with actin to regulate cytoprotective responses to stretching. *J. Cell Sci*. 110: 11–21.

Gorlin, J.B., Kwiatkowski, D.J., Biology, C., General, M., Hospital, C., and Division, P.O. 1990. Human endothelial actin-binding protein (ABP-280, nonmuscle filamin): a molecular leaf spring. *J. Cell Biol.* 111: 1089–1105.

Gräter, F., Shen, J., Jiang, H., Gautel, M., and Grubmüller, H. 2005. Mechanically induced titin kinase activation studied by force-probe molecular dynamics simulations. *Biophys. J.* 88: 790–804.

Hart, A. W., Morgan, J. E., Schneider, J., West, K., McKie, L., Bhattacharya, S., Jackson, I.J., and Cross, S. H. 2006. Cardiac malformations and midline skeletal defects in mice lacking filamin A. *Hum. Mol. Genet.* 15: 2457–2467.

Hartwig, J H, Tyler, J., and Stossel, T. P. 1980. Actin-binding protein promotes the bipolar and perpendicular branching of actin filaments. *J. Cell Biol.* 87: 841–848.

Hartwig, John H, and Stossel, T. P. 1975. Isolation and properties of actin, myosin, and a new actinbinding protein in rabbit alveolar macrophages. *J. Biol Chem*. 250: 5696–5705.

Heikkinen, O.K., Ruskamo, S., Konarev, P. V, Svergun, D.I., Iivanainen, T., Heikkinen, S.M., Permi, P., Koskela, H., Kilpeläinen, I., and Ylänne, J. 2009. Atomic structures of two novel immunoglobulin-like domain pairs in the actin cross-linking protein filamin. *J. Biol. Chem*. 284: 25450–25458.

Hock, R. S., and Condeelis, J. S. 1987. Isolation of a 240-kilodalton actin-binding protein from Dictyostelium discoideum. *J. Biol Chem*. 262: 394–400.

Hynes, R. O. 2002. Integrins: bidirectional, allosteric signaling machines. *Cell* 110: 673–687.

Ithychanda, S.S., Das, M., Ma, Y.-Q., Ding, K., Wang, X., Gupta, S., Wu, C., Plow, E.F., and Qin, J. 2009. Migfilin, a molecular switch in regulation of integrin activation. *J. Biol. Chem*. 284: 4713–4722.

Ithychanda, S.S., Hsu, D., Li, H., Yan, L., Liu, D.D., Liu, D., Das, M., Plow, E.F., and Qin, J. 2009. Identification and characterization of multiple similar ligand-binding repeats in filamin: implication on filamin-mediated receptor clustering and cross-talk. *J. Biol. Chem*. 284: 35113–35121.

Johnson, C. P., Tang, H.-Y., Carag, C., Speicher, D. W., and Discher, D. E. 2007. Forced unfolding of proteins within cells. *Science*. 317: 663–666.

Kiema, T., Lad, Y., Jiang, P., Oxley, C.L., Baldassarre, M., Wegener, K.L., Campbell, I.D., Ylänne, J., and Calderwood, D.A. 2006. The molecular basis of filamin binding to integrins and competition with talin. Mol. *Cell* 21: 337–347.

Kley, R.A, Serdaroglu-Oflazer, P., Leber, Y., Odgerel, Z., Van der Ven, P.F.M., Olivé, M., Ferrer, I., Onipe, A., Mihaylov, M., Bilbao, J.M., Lee, H.S., Höhfeld, J., Djinović-Carugo, K., Kong, K., Tegenthoff, M., Peters, S.A., Stenzel, W., Vorgerd, M., Goldfarb, L.G., and Fürst, D.O. 2012. Pathophysiology of protein aggregation and extended phenotyping in filaminopathy. *Brain* 135: 2642–2660.

Koenderink, G. H., Dogic, Z., Nakamura, F., Bendix, P. M., MacKintosh, F. C., Hartwig, J. H., Stossel, T.P., and Weitz, D. A. 2009. An active biopolymer network controlled by molecular motors. *Proc .Natl. Acad. Sci. U S A*. 106: 15192–15197.

Kovacevic, I., and Cram, E. J. 2010. FLN-1/filamin is required for maintenance of actin and exit of fertilized oocytes from the spermatheca in C. elegans. *Dev. Bio*. 347: 247–257.

Krakow, D., Robertson, S. P., King, L. M., Morgan, T., Sebald, E. T., Bertolotto, C., Wachsmann-Hogiu, S., Acuna, D., Shapiro, S.S., Takafuta, T., Aftimos, S., Kim, C.A., Firth, H., Steiner, C.E., Cormier-Daire, V., Superti-Furga, A., Bonafe, L., Graham, J.M. Jr., Grix,A., Bacino, C.A., Allanson, J., Bialer, M.G., Lachman, R.S., Rimoin, D.L., and Cohn, D. H. 2004. Mutations in the gene encoding filamin B disrupt vertebral segmentation, joint formation and skeletogenesis. *Nat. Genet*. 36: 405–410.

Kuhlman, P. A., Hemmings, L., and Critchley, D. R. 1992. The identification and characterisation of an actin-binding site in alpha-actinin by mutagenesis. *FEBS Lett.* 304: 201–206.

Kyndt, F., Gueffet, J.-P., Probst, V., Jaafar, P., Legendre, A., Le Bouffant, F., Toquet, C., Roy, E., McGregor, L., Lynch, S. A., Newbury-Ecob, R., Tran, V., Young, I., Trochu, J.N., Le Marec, H., and Schott, J.J. 2007. Mutations in the gene encoding filamin A as a cause for familial cardiac valvular dystrophy. *Circulation* 115: 40–49.

Lad, Y., Jiang, P., Ruskamo, S., Harburger, D.S., Ylanne, J., Campbell, I.D., and Calderwood, D. A. 2008. Structural basis of the migfilin-filamin interaction and competition with integrin tails. *J. Biol. Chem.* 283: 35154–35163.

Lad, Y., Kiema, T., Jiang, P., Pentikäinen, O.T., Coles, C.H., Campbell, I.D., Calderwood, D. A, and Ylänne, J. 2007. Structure of three tandem filamin domains reveals auto-inhibition of ligand binding. EMBO J. 26: 3993–4004.

Lee, S. H., and Dominguez, R. 2010. Regulation of actin cytoskeleton dynamics in cells. *Mol. Cells*. 29: 311–325.

Leung, R., Wang, Y., Cuddy, K., Sun, C., Magalhaes, J., Grynpas, M., and Glogauer, M. 2010. Filamin A regulates monocyte migration through Rho small GTPases during osteoclastogenesis. *J Bone Miner. Res*. 25: 1077–1091.

Li, M., Bermak, J. C., Wang, Z. W., and Zhou, Q. Y. 2000. Modulation of dopamine D(2) receptor signaling by actin-binding protein (ABP-280). *Mol. Pharmacol.* 57: 446–452.

Li, M. G., Serr, M., Edwards, K., Ludmann, S., Yamamoto, D., Tilney, L. G., Field, C.M., and Hays, T. S. 1999. Filamin is required for ring canal assembly and actin organization during Drosophila oogenesis. *J Cell Biol.* 146:1061–1074.

Light, S., Sagit, R., Ithychanda, S.S., Qin, J., and Elofsson, A. 2012. The evolution of filamin - a protein domain repeat perspective. J. Struct. Biol. 179: 289–298.

López, J. A. 1994. The platelet glycoprotein Ib-IX complex. *Blood Coagul. Fibrinolysis.* 5: 97–119.

Lu, J., Lian, G., Lenkinski, R., De Grand, A., Vaid, R. R., Bryce, T., Stasenko, M., Boskey, A., Walsh, C., and Sheen, V. 2007. Filamin B mutations cause chondrocyte defects in skeletal development. *Hum. Mol. Genet.* 16: 1661–1675.

Luan, X., Hong, D., Zhang, W., Wang, Z., and Yuan, Y. 2010. A novel heterozygous deletion-insertion mutation (2695-2712 del/GTTTGT ins) in exon 18 of the filamin C gene causes filaminopathy in a large Chinese family. *NMD*. 20: 390–396.

Meyer, S. C., Sanan, D. A., and Fox, J. E. 1998. Role of actin-binding protein in insertion of adhesion receptors into the membrane. *J. Biol Chem.* 273: 3013–3020.

Meyer, S. C., Zuerbig, S., Cunningham, C. C., Hartwig, J. H., Bissell, T., Gardner, K., and Fox, J. E. 1997. Identification of the region in actin-

binding protein that binds to the cytoplasmic domain of glycoprotein IBalpha. *J. Biol Chem*. 272: 2914–2919.

Moore, S. W., Roca-Cusachs, P., and Sheetz, M. P. 2010. Stretchy proteins on stretchy substrates: the important elements of integrin-mediated rigidity sensing. *Dev. Cell*. 19: 194–206.

Müller, R., Gräwert, M. A, Kern, T., Madl, T., Peschek, J., Sattler, M., Groll, M., and Buchner, J. 2013. High-resolution structures of the IgM Fc domains reveal principles of its hexamer formation. *Proc. Natl. Acad. Sci. U S A*. 110: 10183–10188.

Nakamura, F., Heikkinen, O., Pentikäinen, O.T., Osborn, T.M., Kasza, K.E., Weitz, D. A, Kupiainen, O., Permi, P., Kilpeläinen, I., Ylänne, J., Hartwig, J. H., and Stossel, T. P. 2009. Molecular basis of filamin A-FilGAP interaction and its impairment in congenital disorders associated with filamin A mutations. *PloS One* 4: e4928.

Nakamura, F., Osborn, T.M., Hartemink, C. A., Hartwig, J.H., and Stossel, T.P. 2007. Structural basis of filamin A functions. *J Cell Biol.* 179: 1011–1025

Nakamura, F., Pudas, R., Heikkinen, O., Permi, P., Kilpeläinen, I., Munday, A.D., Hartwig, J.H., Stossel, T.P., and Ylänne, J. 2006. The structure of the GPIb-filamin A complex. *Blood* 107: 1925–1932.

Nakamura, F., Stossel, T.P., and Hartwig, J.H. 2011. The filamins: organizers of cell structure and function. *Cell Adh. Migr.* 5: 160–169

Nikki, M., Meriläinen, J., and Lehto, V.-P. 2002. FAP52 regulates actin organization via binding to filamin. *J. Biol Chem.* 277: 11432–11440.

Page, R. C., Clark, J. G., and Misra, S. 2011. Structure of filamin A immunoglobulin-like repeat 10 from Homo sapiens. *Acta Crystallogr. Sect. F Struct. Biol. Cryst. Commun.* 67: 871–876.

Pentikäinen, U., Jiang, P., Takala, H., Ruskamo, S., Campbell, I. D., and Ylänne, J. 2011. Assembly of a filamin four-domain fragment and the influence of splicing variant-1 on the structure. *J. Biol Chem.* 286: 26921–26930.

Pentikäinen, U., and Ylänne, J. 2009. The regulation mechanism for the auto-inhibition of binding of human filamin A to integrin. *J. Mol. Biol.* 393: 644–657.

Pfaff, M., Liu, S., Erle, D. J., and Ginsberg, M. H. 1998. Integrin beta cytoplasmic domains differentially bind to cytoskeletal proteins. *J. Biol Chem.* 273: 6104–6109.

Playford, M.P., Nurminen, E., Pentikäinen, O.T., Milgram, S.L., Hartwig, J.H., Stossel, T.P., and Nakamura, F. 2010. Cystic fibrosis transmembrane conductance regulator interacts with multiple immunoglobulin domains of filamin A. *J. Biol. Chem.* 285: 17156–17165.

Popowicz, G. M., Müller, R., Noegel, A. A., Schleicher, M., Huber, R., and Holak, T. A. 2004. Molecular structure of the rod domain of dictyostelium filamin. *J. Mol. Biol.* 342: 1637–1646.

Pudas, R., Kiema, T.-R., Butler, P.J.G., Stewart, M., and Ylänne, J. 2005. Structural basis for vertebrate filamin dimerization. *Structure* 13: 111–119.

Puklin-Faucher, E., and Sheetz, M. P. 2009. The mechanical integrin cycle. *J. Cell Sci.* 122: 575–575.

Razinia, Z., Mäkelä, T., Ylänne, J., and Calderwood, D.A 2012. Filamins in mechanosensing and signaling. *Annu. Rev. Biophys.* 41: 227-246.

Ricca, B. L., Venugopalan, G., and Fletcher, D. A. 2013. To pull or be pulled: parsing the multiple modes of mechanotransduction. *Curr. Opin. Cell Biol.* 25: 558–564.

Robertson, S. P., Twigg, S. R. F., Sutherland-Smith, A. J., Biancalana, V., Gorlin, R. J., Horn, D., Kenwrick, S.J., Kim, C.A., Morava, E., Newbury-Ecob, R., Orstavik, K.H., Quarrell, O.W., Schwartz, C.E., Shears, D.J., Suri, M., Kendrick-Jones, J., and Wilkie, A. O. M. 2003. Localized mutations in the gene encoding the cytoskeletal protein filamin A cause diverse malformations in humans. *Nat.genet.* 33: 487–491.

Rognoni, L., Stigler, J., Pelz, B., Ylanne, J., and Rief, M. 2012. Dynamic force sensing of filamin revealed in single-molecule experiments. *Proc. Natl. Acad. Sci.* 21: 1–6.

Rossier, O. M., Gauthier, N., Biais, N., Vonnegut, W., Fardin, M.-A., Avigan, P., Heller, E.R., Mathur, A., Ghassemi, S., Koeckert, M.S., Hone, J.C., and Sheetz, M. P. (2010). Force generated by actomyosin contraction builds bridges between adhesive contacts. *EMBO J.* 29: 1055–1068.

Ruskamo, S., Gilbert, R., Hofmann, G., Jiang, P., Campbell, I. D., Ylänne, J., and Pentikäinen, U. 2012. The C-terminal rod 2 fragment of filamin A forms a compact structure that can be extended. *Biochem. J.* 446: 261–269.

Ruskamo, S., and Ylänne, J. 2009. Structure of the human filamin A actin-binding domain. *Acta Crystallogr. D Biol. Crystallogr.* 65: 1217–1221.

Sawyer, G. M., and Sutherland-Smith, A. J. 2012. Crystal structure of the filamin N-terminal region reveals a hinge between the actin binding and first repeat domains. *J. Mol. Biol.* 424: 240–247.

Seo, M.-D., Seok, S.-H., Im, H., Kwon, A.-R., Lee, S.J., Kim, H.-R., Cho, Y., Park, D., and Lee, B.-J. 2009. Crystal structure of the dimerization domain of human filamin A. *Proteins* 75: 258–263.

Sharma, M., Pampinella, F., Nemes, C., Benharouga, M., So, J., Du, K., Bache ,K.G., Papsin, B., Zerangue, N., Stenmark, H., and Lukacs, G. L. 2004. Misfolding diverts CFTR from recycling to degradation: quality control at early endosomes. *The J Cell Biol.* 164: 923–933.

Shatunov, A., Olivé, M., Odgerel, Z., Stadelmann-Nessler, C., Irlbacher, K., Van Landeghem, F., Bayarsaikhan, M., Lee, H.S., Goudeau, B., Chinnery, P.F., Straub, V., Hilton-Jones, D., Damian, M.S., Kaminska, A., Vicart, P., Bushby, K., Dalakas, M.C., Sambuughin, N., Ferrer, I., Goebel, H.H., and Goldfarb, L. G. 2009. In-frame deletion in the seventh immunoglobulin-like repeat of filamin C in a family with myofibrillar myopathy. *Eur. J.Hum. Genet.* 17: 656–663.

Sjekloća, L., Pudas, R., Sjöblom, B., Konarev, P., Carugo, O., Rybin, V., Kiema, T.R., Svergun, D., Ylänne, J., and Djinović Carugo, K.. 2007. Crystal

structure of human filamin C domain 23 and small angle scattering model for filamin C 23-24 dimer. *J. Mol. Biol.* 368: 1011-1023.

Smith, L., Page, R.C., Xu, Z., Kohli, E., Litman, P., Nix, J.C., Ithychanda, S.S., Liu, J., Qin, J., Misra, S., *et al.* 2010. Biochemical basis of the interaction between cystic fibrosis transmembrane conductance regulator and immunoglobulin-like repeats of filamin. *J. Biol. Chem.* 285: 17166–17176.

Sokol, N. S., and Cooley, L. 1999. Drosophila filamin encoded by the cheerio locus is a component of ovarian ring canals. *Curr. Biol.* 9: 1221–1230.

Sokol, N. S., and Cooley, L. 2003. Drosophila filamin is required for follicle cell motility during oogenesis. *Dev. Biol.* 260: 260–272.

Stossel, T.P., Condeelis, J., Cooley, L., Hartwig, J.H., Schleicher, M., and Shapiro, S.S. 2001. Filamins as integrators of cell mechanics and signalling. *Nat. Rev. Mol. Cell Biol.* 2: 138–145.

Tadokoro, S., Shattil, S. J., Eto, K., Tai, V., Liddington, R. C., de Pereda, J. M., Ginsberg, M.H., Calderwood, D. A. 2003. Talin binding to integrin beta tails: a final common step in integrin activation. *Science* 302: 103–106.

Takala, H., Nurminen, E., Nurmi, S.M., Aatonen, M., Strandin, T., Takatalo, M., Kiema, T., Gahmberg, C.G., Ylänne, J. and Fagerholm, S.C. 2008. Beta2 integrin phosphorylation on Thr758 acts as a molecular switch to regulate 14-3-3 and filamin binding. *Blood* 112: 1853–1862.

Thelin, W. R., Chen, Y., Gentzsch, M., Kreda, S. M., Sallee, J. L., Scarlett, C. O., Borchers, C.H., Jacobson, K., Stutts, M.J., and Milgram, S. L. 2007. Direct interaction with filamins modulates the stability and plasma membrane expression of CFTR. *J. Clin. Invest.* 117: 364–374.

Tossavainen, H., Seppälä, J., Sethi, R., Pihlajamaa, T., and Permi, P. 2014. H(N), N(H), C (α), C (β), and methyl group assignments of filamin multidomain fragments IgFLNc4-5 and IgFLNa3-5. *Biomol. NMR Assign.* (In press)

Tu, Y., Wu, S., Shi, X., and Chen, K. 2003. Migfilin and Mig-2 link focal adhesions to filamin and the actin cytoskeleton and function in cell shape modulation. *Cell.* 113: 37–47.

Van der Ven, P. F., Wiesner, S., Salmikangas, P., Auerbach, D., Himmel, M., Kempa, S., Hayess, K., Pacholsky, D., Taivainen, A., Schröder, R., Carpén, O., and Fürst, D. O. 2000. Indications for a novel muscular dystrophy pathway. gamma-filamin, the muscle-specific filamin isoform, interacts with myotilin. *J. Cell Biol.* 151: 235–248.

Vargas, M., Sansonetti, P., and Guillén, N. 1996. Identification and cellular localization of the actin-binding protein ABP-120 from Entamoeba histolytica. *Mol. Microbiol.* 22: 849–857.

Vorgerd, M., Ven, P. F. M. Van Der, Bruchertseifer, V., Lo, T., Kley, R. A., Schröder, R., Lochmüller, H., Himmel, M., Koehler, K., Fürst, D.O., and Huebner, A. 2005. A mutation in the dimerization domain of Filamin C causes a novel type of autosomal dominant myofibrillar myopathy. *Am. J. Hum. Genet.* 77: 297–304.

Wang, N., Tytell, J. D., and Ingber, D. E. 2009. Mechanotransduction at a distance: mechanically coupling the extracellular matrix with the nucleus. *Nat. Rev. Mol. Cell Biol.* 10: 75–82.

Williamson, D., Pikovski, I., Cranmer,S.L., Mangin, P., Mistry, N., Domagala, T., Chehab, S., Lanza, F., Salem and H. H., Jackson, S. P. 2002. Interaction between platelet glycoprotein Ib alpha and filamin-1 is essential for glycoprotein Ib/IX receptor anchorage at high shear. *J. Biol. Chem.* 277: 2151-2159.

Wurzburg, B.A., and Jardetzky, T.S. 2009. Conformational flexibility in immunoglobulin E-Fc 3-4 revealed in multiple crystal forms. *J. Mol. Biol.* 393: 176–190.

Xie, Z., Xu, W., Davie, E. W., and Chung, D. W. 1998. Molecular cloning of human ABPL, an actin-binding protein homologue. *Biochem. Biophys. Res. Commun.* 251: 914–919.

Xu, B. W., Xie, Z., Chung, D. W., Davie, E. W., and Gp, G. 1998. A novel human actin-binding protein homologue that binds to platelet glycoprotein Ibalpha. *Blood* 92: 1268–1276.

Zenker, M., Rauch, A., Winterpacht, A., Tagariello, A., Kraus, C., Rupprecht, T., Sticht, H., and Reis, A. 2004. A dual phenotype of periventricular nodular heterotopia and frontometaphyseal dysplasia in one patient caused by a single FLNA mutation leading to two functionally different aberrant transcripts. *Am. J. Hum. Genet.* 74: 731–737.

Zhou, A.-X., Hartwig, J.H., and Akyürek, L.M. 2010. Filamins in cell signaling, transcription and organ development. *Trends Cell Biol.* 20: 113–123.

Zhou, X., Tian, F., Sandzén, J., Cao, R., Flaberg, E., Szekely, L., Cao, Y., Ohlsson, C., Bergo, M.O., Borén, J., and Akyürek, L. M. 2007. Filamin B deficiency in mice results in skeletal malformations and impaired microvascular development. *Proc. Natl. Acad. Sci.* U S A. 104: 3919–3924.